

Comprehensive Summaries of Uppsala Dissertations
from the Faculty of Medicine 1382



Morphometrical Methodology in Quantification of Biological Tissue Components

BY

BO BLOMGREN



ACTA UNIVERSITATIS UPSALIENSIS
UPPSALA 2004

Dissertation presented at Uppsala University to be publicly examined in Rosénsalen, Akademiska sjukhuset, Uppsala, Friday, November 19, 2004 at 09:15 for the degree of Doctor of Philosophy (Faculty of Medicine). The examination will be conducted in English.

Abstract

Blomgren, B. 2004. Morphometrical Methodology in Quantification of Biological Tissue Components. Acta Universitatis Upsaliensis. *Comprehensive Summaries of Uppsala Dissertations from the Faculty of Medicine* 1382. 63 pp. Uppsala. ISBN 91-554-6068-2

Objective:

To develop and validate computer-assisted morphometrical methods, based on stereological theory, in order to facilitate the analysis and quantitative measurements of biological tissue components.

Material and methods:

Biopsy specimens from the vaginal wall or from the vestibulum vaginae of healthy women, or from women suffering from incontinence or vestibulitis were used.

A number of histochemical methods for light microscopy were used, and modified for the different morphometrical analyses. Electron microscopy was used to reveal collagen fibre diameter.

Computer-assisted morphometry, based on image analysis and stereology, was employed to analyse the different tissue components in the biopsies. Computer programs for these purposes were developed and validated.

Results:

The results show that computer-assisted morphometry is of great value for quantitative measurements of the following tissue components:

Epithelium: The epithelial structure, instead of just thickness, was measured in an unbiased way.

Collagen: The collagen fibril diameter was determined in electron microscopic specimens, and the collagen content was analysed in light microscopic specimens.

Elastic fibres: The amount of elastic fibres in the connective tissue was measured after visualisation by autofluorescence.

Vasculature: A stereological method using a cycloid grid was implemented in a computer program. Healthy subjects were compared with patients suffering from vestibulitis. The results were identical in the two groups.

Smooth muscle: A stereological method using a point grid was implemented in a computer program. Using the Delesse principle, the fibres were calculated as area fractions. The area fractions were highly variable among the different specimens.

Conclusion:

Morphometry, used correctly, is an important analysis method in histopathological research. It is important that the methods are as simple and user-friendly as possible. The present studies show that this methodology can be applied for most quantitative histological analyses.

Keywords: Morphometry, Stereology, Image analysis, histology

Bo Blomgren, Department of Women's and Children's Health, Uppsala University, SE-75185 Uppsala, Sweden

© Bo Blomgren 2004

ISSN 0282-7476

ISBN 91-554-6068-2

urn:nbn:se:uu:diva-4628 (<http://urn.kb.se/resolve?urn=urn:nbn:se:uu:diva-4628>)

To my family

List of Papers

This thesis is based on the studies reported in the following original papers, which will be referred to by their Roman numerals (I – V).

I Falconer C., Blomgren B., Johansson O., Ulmsten U., Malmström A., Westergren-Thorsson G. and Ekman-Ordeberg G.

Different organization of collagen fibrils in stress-incontinent women of fertile age

Acta Obstetrica et Gynecologica Scandinavica 1998, 77, 87-94

II Blomgren B., Bohm-Starke N., Falconer C. and Hilliges M.

A computerised stereological method for quantitative estimation of surface area of blood vessels

Image Analysis and Stereology 2001, 20, 129-132

III Blomgren B., Falconer C., Roomans G., Ulmsten U. and Hilliges M.

A novel method for visualisation of elastic fibres – suitable for image analysis and morphometry

Image Analysis and Stereology 2001, 20, 522-526

IV Blomgren B., Johannesson U., Bohm-Starke N., Falconer C. and Hilliges M.

A computerised, unbiased method for epithelial measurement

Micron 2004, 35, 319-329

V Blomgren B., Falconer C., Hilliges M., and Roomans G. M.

The structure of the normal vaginal wall as revealed by morphometry

Submitted

Contents

Introduction.....	9
The history of morphometry	9
Classical geometry	9
Mathematical modelling and probability theory	10
What is morphometry?	13
Image processing – a short note.....	13
Stereology	13
Image analysis	13
Features to measure with morphometry	15
Terminology	16
What can morphometry be used for?.....	16
Gynaecology - The vaginal wall	17
Anatomy	18
Histology	19
Aim of the study.....	21
Specific aims of studies I to V	21
Methods	22
The sampling procedure – overview	22
The histotechnical procedure.....	23
The histochemical staining procedures	24
The immunohistochemical staining procedure.....	25
Stereological considerations.....	25
Stereological considerations in the different studies	26
Image analysis.....	27
Image enhancement	27
Image segmentation and thresholding	28
Image measurements	28
Image analysis strategies in the different studies	28
Statistical interpretation of data.....	30
Results.....	32
Results regarding the developed methods: Study II, III & IV.....	32
Epithelium: Study IV & V	33
Collagen: Study I & V.....	34

Vasculature: Study II.....	34
Elastic fibres: Study III & V.....	35
Smooth muscle: Study V.....	35
Discussion.....	36
Discussion of development of methods.....	36
Participants	36
Sampling and stereology.....	36
Histology and staining technology	37
Image analysis	38
Discussion of the findings in the different experimental setups.....	39
Future perspectives.....	42
Conclusion	43
Figures	45
Acknowledgements.....	50
References.....	52
Appendix.....	57
Appendix 1 Staining methods.....	57
Haematoxylin and Eosin (Harris)	57
Weigerts elastin (without Van Gieson counterstain)	57
Massons trichrome.....	58
Sirius red.....	58
Appendix 2 Computer program flowcharts	59

Abbreviations

2-D	Two-dimensional
3-D	Three-dimensional
ABC	Avidin-Biotin Complex
AF	AutoFluorescence
B.C.	Before Christ
BLS	Distance from Basal Layer to Surface
CCD	Charge-Coupled Device
D_{\min}	Minimum Diameter
DP	Dermal Papilla
DPD	inter-Dermal Papilla Distance
DPS	Distance from Dermal Papilla to Surface
DPW	Dermal Papilla Width
fVIII	Coagulation factor VIII
FSU	Fundamental Sampling Unit
GLP	Good Laboratory Practice
GOP [®]	Graphic Operation Processing
H & E	Haematoxylin and Eosin
IHS	Intensity-Hue-Saturation colour space
M3C	Massons TriChrome stain
NBF	Neutral Buffered Formaline
Pixel	Picture Element
RGB	Red-Green-Blue colour space
ROI	Region Of Interest
SEM	Standard Error of Mean
SR	Sirius Red
SUI	Stress Urinary Incontinence
TEM	Transmission Electron Microscope
UR	Uniform Random sampling method
UV	UltraViolet

Introduction

The history of morphometry

Classical geometry

The ancient Egyptians were the first to use the basic geometrical principles. About 6000 years ago, the Egyptians living near the Nile employed measurements of surface area in order to calculate their land areas. For this purpose, they marked the land boundaries with ropes, whose length, and thereby the area inside, was measured and calculated. These early civilisations were among the first humans to use geometrical solutions to solve practical problems.

The Egyptians may have been the inventors of geometry, but the first to use it in a broader manner were the Greeks. The famous Greek mathematician Pythagoras (582 – 500 B.C.) invented the Pythagorean theorem, one of the best known concepts of classical geometry. The Greeks used geometrical principles in their architecture; gardens, amphitheatres, gymnasiums, roads, wagons and sailing vessels.

Greece became the architectural and academic centre of the world. Euclid (330 – 275 B.C.), another of the famous Greek mathematicians, made important contributions to the use of geometry. His great work *Elementa*, considered to be among the best scientific handbooks ever written, deals with planar as well as spatial geometry and number theory. The classical Euclidean geometry provides tools for construction of geometric objects and for the understanding of mathematical relationships. These approaches cannot, however, be applied in biology, since biological structures show large variation and do not fit in the models of classically shaped objects. The extent of the variation depends on the actual geometric features of the objects and the degree of variation between objects in the population. Therefore, applying classical geometrical formulas to biological objects will introduce bias due to their variable nature.

Before unbiased stereology (Baddeley, 1993) was invented in the 1980s, the morphometrical methods used for quantification of for example tissue sections in histology consisted of assumption- and model-based methods built on classical geometry (Aherne and Dunnill, 1982).

Mathematical modelling and probability theory

There is no evidence that any morphometrical or stereological methods were developed until the classical Greek mathematics were rediscovered during the renaissance. Starting in the fifteenth century, however, a number of contributions established the theoretical foundations for morphometry.

In the Habsburg empire (today Italy), the mathematician Buonaventura Francesco Cavalieri (1598 – 1647) (Ghosh, 1998) became inspired by the works of Euclid, and applied geometrical theorems to practical problems. After having met Galileo, he later became a pupil of the famous astronomer, and started experiments with geometrical models in astronomy. Cavalieri worked and wrote on trigonometry, optics and astronomy. He also worked on a number of problems of motion, and published some books on astrology.

The discovery that made him famous in morphometrical science was made in 1635. Cavalieri then showed that the mean volume of a randomly shaped object could be estimated in a theoretically unbiased manner from the sum of areas and the thickness of the sections cut through the object. This was a step away from the classical geometry he had been studying. It is today the most common method for estimating reference volume. Other methods that might be suitable for measurement of a reference volume are simple weighing, if the density of the organ or tissue is known, or volumetry. Volumetry using water replacement relies upon the Archimedean principle of fluid displacement. It can be used in many cases without problems, but for very small volumes, and for tissues that absorb water, it is not the method of choice. Application of the Cavalieri method for volume estimation is very straightforward. If the position of the first section cut in the object is uniformly random and all sections cut through it are of the same thickness, then the equations are unbiased estimators of the volume of the object.

The French mathematician Georges Louis Leclerc, Comte de Buffon (1707 – 1788) studied probability and also mechanics, geometry, number theory and differential and integral calculations (Browne, 1988). His most important contribution to morphometry, and also his most famous mathematical experiment, is the needle problem. In the year 1777 he proposed and correctly solved the problem, which originally was an experiment for calculating π .

The formulation of the problem is: ‘Parallel lines, d units apart, are ruled on a plane surface. A needle of length l (where $l < d$) is thrown *at random* on the plane. What is the probability that it will meet one of the parallel lines?’ In practice, Buffon threw sticks over his shoulder on a tiled floor and counted the number of times the sticks fell across the lines between the tiles. He could see that a needle tossed at random onto a grid of lines intersects each line with a probability directly proportional to the length of the needle. This experiment was widely discussed among mathematicians, and it actually inaugurated a new branch of mathematics, today known as the theory of *geometrical probability*. This theory now provides much of the foundation on which morphometry rests. The principle of this experiment became the theoretical basis for estimating length and surface area of randomly shaped objects.

Achille Ernest Oscar Joseph Delesse (1817 – 1881) was a French geologist and mineralogist and one of his main interests was the determination of the composition of rocks (Royet, 1991). He invented a method to measure the amount of a particular mineral in a rock. First, he cut it through, polished the exposed face and covered the face with waxed paper. It is important to realise that a polished plane of a rock can be considered an infinitely thin section, as opposed to histopathological sections. Delesse thereafter traced the exposed portions (phases) of the mineral of interest with a pencil on the paper. Subsequently, he weighed the paper, cut out the mineral traces and weighed them. The ratio of the weights gave the proportion of the surface covered by the mineral. However, Delesse wanted to quantify the relationship between the phase area on the polished face from the rock and the total phase volume in the whole rock. He then compared the phase areas on polished rock faces with the total phase volume in the specimen. It was evident that the total area of a phase on each cut surface is proportional to the total phase in the entire rock.

Today, the Delesse principle provides the basis for estimating the volume of randomly shaped objects based on their profile areas on random sections in a number of disciplines including mineralogy, metallurgy and biology.

S. D. Wicksell, a Swedish mathematician, published an article on a statistical problem in anatomical science in the year 1925 (Wicksell, 1925). The problem was to estimate the distribution function of tumour sizes in cross-sectioned spleens of animals suffering from cancer. The tumours were assumed to be spherical, and when the spleens were cut into two-dimensional slices, the tumour profiles were circular. The relation between the distribution of the tumour radii and the distribution of the radii of the observable spheres was then derived.

In another study, Wicksell tried to estimate the number of follicles in the thyroid gland. Sections of thyroid tissue were cut, and subsequently reconstructed in three dimensions. It was then evident that the number of follicles in a specified volume of thyroid tissue could not be estimated from the number of follicle profiles on the cut sections. This became known as the “corpuscle problem”. Many mathematicians and other scientists have since then tried to overcome the problem by use of different “correction formulas”. These attempts have only added further bias since the models and assumptions can be used for theoretical objects, but are useless for biological objects with random shapes.

The volume of the tumours in the spleens could be measured quite easily, since their growth pattern in the soft splenic tissue gave them rounded shapes. The thyroid follicles, however, were not at all rounded, but had instead “random shapes”.

The conclusion of these experiments was that accurate estimates of the number of biological objects with arbitrary, random sizes and shapes cannot be obtained from histological sections using assumption-based morphometry.

The disector principle was invented by D. C. Sterio (pseudonym for a well-known Danish stereologist) in 1984 (Sterio, 1984). This was the first true unbiased method for particle counting in a specified tissue volume. No assumptions had to be made about the particles’ size, shape or orientation in the specified tissue region.

The design of disector method made it possible to overcome the corpuscle problem without the use of assumptions or correction factors.

The disector method is used for unbiased estimates of the number of discrete objects in a defined reference space. The disector consists of a pair of serial sections a known distance apart. If the transect of an object is seen in one section but not in the next, it is counted (Fig. 1).

The invention of the disector principle was a breakthrough for methods of quantitative morphological analysis. These methods could in theory overcome the most severe forms of bias introduced by slicing three-dimensional objects into two-dimensional sections. Today, a number of unbiased stereological methods has been developed for making efficient estimates of average or total quantities such as total number, average particle volume etc (Gardella et al. 2003; Møller et al. 1990).

What is morphometry?

The term *morphometry* is derived from the Greek, and means “measurement of form”. In biology, it is the science of measurement of forms in tissue (Weibel, 1967). This means to measure area, perimeter, length and number... Biological morphometry is not a new science. After the invention of the microscope around 1610 (Purcell, 1974), scientists soon wanted to perform quantitative analyses on the different parts of tissue they were seeing. Before the invention of modern stereology (see below), the morphometrical methods relied on classical Euclidean geometry. They are said to be *assumption-based*, and therefore also biased. Tissue elements are fitted into classical geometric bodies. Cells, for example, are assumed to be spheres.

Today, the term *morphometry* can be used as a common name for *stereology* and *image analysis*.

Image processing – a short note

The distinction between *image processing* and *image analysis* lies in the extraction of information from the image that is done in the image analysis process (Russ, 1995). Image processing is a rearrangement of the image to get it more suitable, either for subsequent measurements – the analysis process – or simply to make it better for publication or some other type of communication.

Stereology

Stereology is the science dealing with the geometrical relationships between 3-dimensional objects existing in the real world, and images or sections of these visualised in 2-D (Howard and Reed, 1998). Stereology has found its most common use in microscopical imaging. This includes light microscopy of different kinds, from conventional brightfield to fluorescence and confocal microscopy. It is also useful for electron microscopy. However, the stereological methods used for microscopical analysis are also appropriate for use in the macroscopic world. In modern stereology, a collection of unbiased methods and tools are employed for the analysis of the three-dimensional structures in 2-D, for example measurements of blood vessel volume from histological sections.

Image analysis

The technique for computerised image analysis was introduced in the 1970:s after the development of microcomputers. The computer as expert for bio-

logical quantification was believed to give a higher degree of objectivity than human analysis in the interpretation of morphological data (Russ, 1995).

Image analysis is a technique that mainly deals with images and image information. In image analysis, the main goal is to perform operations on images that have been fed into the computer, i.e. digitised images. The basic problem is to determine the pixel structure in the image and to manipulate the pixels. A primary goal is to threshold the image into two components, namely objects of interest and other structures, the background. When the image is in this state, it is a segmented binary image. After thresholding of the image, it is often a very simple procedure to perform measurements on it. The key problem of image analysis is to create reproducible and accurate filtering and segmentation methods for every image analysis project. In certain areas of application, such as metallurgy and geology, this can be a simple task, and the images can be segmented based only on grey level intensity. In almost all biomedical applications, however, and especially in histology, the images are almost always of low and variable contrast. The development of reliable segmentation techniques for these types of images is the major problem of image analysis. The so-called classical filtering algorithms are unable to overcome all the problems with segmenting biological images. Examples of classical edge- and line detectors are Sobel, Prewitt and Laplace algorithms.

Contextual image analysis

In conventional image analysis, every pixel is assumed to have a particular significance, e.g. that the grey level intensity or the colour information in a single pixel determines its relevance to the image as a whole.

The introduction of the GOP[®] technology (Hedlund et al. 1982; Knutsson, 1982) for contextual image analysis has provided image processing and analysis with a number of new and efficient tools for filtering and segmentation (Fig. 2). These tools can detect and measure texture and structure in images. This is done by implementing *kernels*, squares of pixels of different size that also take the pixels in the *neighbourhood* into consideration. For many situations, often regarding histopathological images, this method is preferred. These images have complex structures and often low contrast, and the significance of the individual pixels is often realised only when looked upon in their contextual environment.

The GOP[®]-operations used in this thesis are the following (Fig. 3):

- Orient
- Phase
- Line

Orient, the *local orientation estimation*, produces an output vector for every neighbourhood. The angle of this vector represents an estimation of the dominant orientation of the oriented structures. The length of the vector, the magnitude value, is a measure of the local energy, either *isotropic* or *oriented* (e.g. the strength of the dominating structure) or a mixture of both. The Orient operation is used in study II (Fig. 4a & b).

Phase is the tool for estimation of the phase of lines and edges in the image. This means that the position of the pixels on the line or edge-like structure is estimated. This operation can use a contextual image produced by the Orient operation. This image then contains an estimate of the dominant orientation. The output argument value from the Phase operation represents the phase estimate. The magnitude value indicates the local directional energy in every neighbourhood (Fig. 4c). The Phase operation is used in study II and V.

Line is used to detect line-like structures. For every neighbourhood, this operation produces an output vector. The angle of this vector represents an estimate of the dominant orientation of the line-like structures. This is similar to Orient. The magnitude value indicates the amount of estimated line energy, i.e. the strength of the dominant line structure (Fig. 4d). The Line operation is used in study III and V.

Even after segmentation of an image, it may not be suitable for correct 3-D measurements. If the sampling technique or the measurement methods are incorrect, the data gained from the image analysis will be useless. Therefore, stereological sampling design and stereological measurement tools must be used also in totally automatised image analysis systems.

Features to measure with morphometry

The basic elements of a 3-D structure in biological tissue are the following (Howard and Reed, 1998):

Three-dimensional objects with a volume, i.e. particles. Cells, fibres, bones and blood vessels are examples of such objects.

Two-dimensional surfaces with an area. The skin surface, surfaces of the 3-D objects mentioned above and membranes are examples of 2-D objects. In fact, membranes actually *have* a thickness, and are

three-dimensional, but since their lateral extent is much larger than their thickness, they are often regarded as being essentially 2-D.

One-dimensional features, essentially lines, possessing length but not width or volume. Examples in biological tissue consists of objects with a negligible lateral dimension compared to their length. Such objects are for example collagen and elastic fibres, axonal networks and blood vessels. Note that all these features actually have three dimensions in a strict mathematical sense, but can be regarded as 1-D depending on the magnification. This means that they can be treated as 3-D objects at a high magnification, but as 1-D lines at a low magnification.

Zero-dimensional objects; points in space. Ideal points in biological tissue can be junctions of 1-D structures, such as bifurcations of blood vessels or branching of fibres. They can also be intersections of 1-D objects with surfaces.

Terminology

In stereology, the terminology is a mixture of terms from statistics and sampling theory, see Table 1.

<i>Term</i>	<i>Meaning</i>
Parameter	Population value estimated in a sample
Sample	Individuals taken from the population and analysed
Estimator	Probe for estimation of a parameter
Estimate	Parameter from an estimator in a random sample
Reference space	A bounded region containing the volume of interest
Expected value	The value expected to be true, for a parameter, among the population

Table 1. *Selected stereological parameters and their meaning.*

What can morphometry be used for?

Morphometry can be used to solve most of the problems commonly encountered by almost all scientists using microscopes (Gundersen et al. 1988). It can also be used in some other fields. Morphometry is the method of choice when a volume of any kind shall be examined (Roberts et al., 1993). Common examples from biological research are livers (Aguila, 2003) or brains (Pakkenberg and Gundersen, 1988), in material science a piece of aluminium (Karlsson and Cruz-Orive, 1991) and in mineralogy a polished rock. In all of

these cases, the interesting feature is the inner structure in the respective objects. Commonly, this structure is beyond the resolution capacity of the eye, and different kinds of microscopes are therefore employed to visualise it.

To achieve a qualitative image of the structure it can be sufficient to make one or a few sections, choose some interesting areas and examine them. Possibly, the examiner only looks through the microscope and registers the findings. This is common procedure in histopathological routine diagnostics. Sometimes the pathologist may take representative images through the microscope.

If a quantitative study is to be made, that study must be planned with a more careful approach.

As mentioned above, it is essential that the study be conducted with great accuracy. When planning quantitative studies in biological research, the following must be considered:

- Is the macroscopic specimen representative for the population?
- Is the microscopic specimen representative for the macroscopic specimen?
- Are the measurements performed on the microscopic specimen *specific* and *sensitive* enough?
- Are the measurements usable with respect to the questions and aim of the study?
- Are the measurements reproducible?

Gynaecology - The vaginal wall

Despite the fact that the vagina, and the vaginal wall, has several important functions (Wei and DeLancey, 2004), such as the female organ of copulation and the canal of childbirth, a thorough morphological description of this organ is currently lacking. There are few descriptions, and little information about basic structural changes in this organ during the life cycle of a woman (Wilkinson, 1992; Fu. et al., 1995; Boreham et al., 2002; Jondet and Dehenin, 2003). There are also few descriptions about changes that can be the case of, for example, urinary incontinence and prolapse (Falconer et al. 1994; Falconer et al. 1998).

There are few systematic long-term studies about pre- and postmenopausal changes in the vagina. Recent studies have shown that the anterior vaginal wall plays an important role in pelvic organ support. In particular the ure-

thra, and the anterior vaginal wall is hence of crucial interest for maintaining continence (Ulmsten and Falconer, 1999; Papa Petros and Ulmsten, 1997; Ulmsten, 1997).

Anatomy

The vagina is a thin-walled musculomembranous tubular organ, about 8 – 9 cm in length (Moore, 1982; Nichols and Randall, 1983; Reiffenstuhl et al., 1975). The anterior wall is normally about 6 – 8 cm long, and the length of the posterior wall is about 7 – 10 cm. The vagina forms the inferior portion of the female genital tract, and serves as the inferior end of the birth canal. It extends from the vestibule, which is the area between the labia minora, and ends at the level of the cervix of the uterus (Fig. 5). The wall consists anatomically of three quite distinct layers:

- The mucosa
- The intermediate muscular layer
- The outer adventitia

The mucosa is lined with a non-keratinised squamous epithelium towards the lumen, and a fibrous – elastic connective tissue. The epithelium does not comprise any glands or hair follicles. The surface of the vaginal mucosa is lubricated by mucus from the cervix and other surrounding glands. Commonly, a longitudinal fold can be seen in the mucosa, on the anterior and posterior walls. These *columnae rugarum* represent the fusion line of the two Müllerian ducts. From the *columnae rugarum* originate transversal folds, *rugae vaginales*. These folds are partly responsible for the considerable distension that the vagina can undergo during childbirth. The rugae appear first after puberty, and become flattened after the menopause.

The connective tissue layer consists of a relatively compact collagenous tissue, with intermingled elastic fibres.

The vaginal spatium is only potential, as the anterior and posterior walls normally are in apposition.

Blood and lymph supply

The arterial blood supply of the vagina comes from the *vaginal arteries*, the vaginal branch of the *uterine artery*, the *internal pudendal artery* and the vaginal branches of the *middle rectal artery*. All these are branches of the *internal iliac arteries* (Fig. 5).

The venous drainage is made up of the *vaginal venous plexuses* along the sides of the vagina. The plexuses are drained through the vaginal veins or the uterine venous plexuses into the *internal iliac veins*.

The lymph drainage comprises three groups of vessels:

1. The lymph vessels from the superior part of the vagina accompany the uterine artery and drain into the *internal* and *external iliac lymph nodes*.
2. The vessels from the middle part of the vagina accompany the vaginal artery and drain into the *internal iliac lymph nodes*.
3. Those from the vestibular area drain mainly into the *superficial inguinal lymph nodes*, but some vestibular vessels drain into the *sacral* and *common iliac lymph nodes*.

Innervation

The nerves of the vagina are derived from the *uterovaginal plexus* which lies in the base of the broad ligament on each side of the supravaginal part of the uterine cervix. Sympathetic, parasympathetic and afferent fibres pass through this plexus. The lower nerve fibres from this plexus supply the cervix and the superior part of the vagina. The *vaginal nerves* follow the vaginal arteries and end in the vaginal wall (Hilliges et al., 1995).

Histology

The vaginal wall consists of the following layers, counted from the lumen and outwards (Ross and Romrell, 1989):

1. The epithelium.
2. The lamina propria, consisting of moderately dense connective tissue.
3. The smooth muscle layer.
4. The adventitia, consisting of a thin layer of connective tissue.

See Fig. 6.

The principal layers, the epithelium, the connective tissue and the smooth muscle layer, are easily recognised in cross sections through the vaginal wall.

The epithelium and lamina propria are commonly put together and referred to as the *mucosa*.

The *epithelium* is a non-keratinised stratified squamous epithelium. The epithelium is divided into basal cell-, transitional cell- and the spinous or prickle cell layers. These layers are sometimes also referred to as basalis, intra-epithelialis and functionalis. The epithelial thickness is determined by the functional status of the ovaries. A striking feature of this epithelium is that the cells in the transitional cell layer are loaded with glycogen, which gives them a swollen, pale appearance in histological sections (Fig. 7). The epithelium is responsive to sex hormones (Voipio et al., 2002). The superficial cells, the cells in the *stratum spinosum*, often contain large keratin granules. In primates, such as humans, the epithelium normally lacks the *stratum*

corneum. Therefore, nuclei are seen throughout the whole thickness of the epithelium. However, in elderly women or in women suffering from prolapse minimal keratinisation is sometimes present. In this situation, the vaginal wall is exposed to air and the superficial cells do keratinise like those in the epidermis, but most often to a lesser extent (Fig. 8) (Nilsson et al., 1995). The vaginal epithelium is somewhat thicker than the cervical epithelium, and the dermal papillae protruding up from the underlying connective tissue are, when present, often considerably larger. There are some reports indicating that these papillae are more numerous on the posterior wall and near the vaginal orifice.

The lamina propria consists of a moderately dense connective tissue (De Lancey and Ashton-Miller, 2004), made up of collagen fibres (collagen I) with intermingled elastic fibres crossing from the basal lamina to the underlying smooth muscle layer. The connective tissue in the lamina propria consists of two distinct regions. The outer region is made up of moderately dense connective tissue. It becomes less dense towards the smooth muscle layer, and in the transitional zone it contains numerous large venules and veins. This deeper and less dense part of the lamina propria can be considered as submucosa.

The collagen fibres are produced by the fibroblasts (Minamitani et al., 2004). Collagen is the most abundant protein in the human body and the dominating structure of the connective tissue. At present, at least 19 different types of collagen are known (Van der Rest and Garrone, 1991, Prockop and Kivirikko, 1995). The main collagen types in fibrous connective tissue are the fibrillar collagens I & III (Van der Rest & Garrone, 1991).

Some of the elastic fibres (Albert et al., 2004) extend into the muscle layer. Some 60 -100 μm below the basement membrane, the elastic fibres usually form an elastic membrane. They have, however, been noted as deep as 300 μm below the basal lamina (Blomgren, unpublished results).

The smooth muscle layer is organised in two, often indistinct, intermingling smooth muscle layers (Hameed, 2003; Morgan, 2003), an outer longitudinal layer and an inner circular layer. Striated muscle fibers from the bulbospongiosus muscle are present at the vaginal opening

The vaginal adventitia is organised into an inner dense connective tissue layer, adjacent to the muscularis, and an outer loose connective tissue layer that blends with the adventitia of the surrounding structures.

Aim of the study

The aim of this study was to develop new, efficient and unbiased morphometrical methods that utilise stereological as well as image analysis technology. It was also to apply the morphometrical technology and newly developed computer-assisted methods to a descriptive analysis of the composition of a tissue.

The aim was in addition to employ these methods to perform a mapping and quantitative description of the anatomical and histological properties in the vaginal wall. The new morphometrical methods were considered necessary to assess the different tissue components, since diameters, area fractions, area per volume and intensity measurements were to be performed. Important structures to investigate were, among others, the connective tissue, including fibres and macromolecules, above all collagen and elastin. Other important investigations were the structure and thickness of the epithelial lining, the vasculature and the amount of smooth muscle tissue.

Specific aims of studies I to V

Study I: To develop a computer-assisted method able to measure the minimum diameter of collagen fibrils. To test the hypothesis that stress urinary incontinence in women is correlated to changes in the paraurethral connective tissue ultrastructure.

Study II: To perform quantitative estimates of the surface area of blood vessels in the vestibulum. A stereology-based computerised method that utilised virtual cycloid grids was developed.

Study III: To apply the recent discovery that elastic fibres show autofluorescence when viewed in UV light. To develop a method for measurement of elastic fibres revealed by their autofluorescence.

Study IV: To develop and evaluate a standardised method for unbiased measurements of epithelial thickness and structure taking the variability of the dermal papillae in consideration.

Study V: To carry out a histological overview of the human vaginal wall, using standardised computer-assisted morphometrical methods, in order to serve as a base for future morphological investigations of this organ.

Methods

The sampling procedure – overview

In the studies included in this thesis, a number of sampling procedures were used. Specimens from different parts of the vaginal wall were used (study I, III - V), as well as from the vestibulum vaginae (study II). The surgical procedure was somewhat different, and the sampling regime was also determined when the separate studies were planned, and the study plan created.

In fig. 9, the biopsy sampling sites are outlined.

Study I:

Six randomly chosen women from the *incontinent* group (n=15) and six from the *control* group (n=16) were biopsied for transmission electron microscopic examination. Punch biopsies with a diameter of 6 mm and a mean weight of 40 mg were taken transvaginally from a position of 6-8 mm lateral to the external orifice of the urethra and to a depth of 10-12 mm.

Study II:

Ten healthy women and ten women suffering from vestibulitis were included in the study. All women were in the same menstrual state, and punch biopsies of 6 mm in diameter were taken from the area around the right Bartholin gland. When the biopsies were embedded in paraffin, care was taken to preserve the correct orientation, so the sections cut became as vertical as possible. This is a prerequisite for the stereological method employed in this study.

Study III:

Ten healthy women were included in the study. Each biopsy was taken transvaginally from a position of 6-8 mm lateral to the external orifice of the urethra and to a depth of 10-12 mm. When the biopsies were embedded in paraffin, care was taken to preserve the correct orientation, so the sections became as vertical as possible. From each paraffin block, two consecutive sections were cut and placed on slides. One slide was stained with Weigerts elastin stain, the other deparaffinised, mounted and covered with coverslips, but left unstained.

Study IV:

Biopsies from the anterior vaginal wall of twelve healthy women were included in the study. As in the previous studies, every effort was made to obtain vertical sections. In this study, it was also of great importance that the epithelium was cut to full thickness, so that the profiles of the dermal papillae would represent the actual situation regarding epithelial thickness and dermal papillae.

Study V:

Biopsies from the anterior vaginal wall of ten healthy women were examined. The biopsies were taken from the apical part of the anterior vaginal wall during hysterectomy for non-malignant conditions. The biopsies comprised the entire vaginal wall, from the epithelial surface to the adventitial lining on the outer surface.

The histotechnical procedure

The studies included in this thesis have used different histotechnical methods. This is due to their specific aims, and what they are supposed to show. The preparation methods used in the studies are listed in Table 2.

<i>Study</i>	<i>Fixation</i>	<i>Staining</i>	<i>Embedding</i>	<i>Mountant</i>	<i>Examination</i>
I	Glutar-aldehyde	Uranyl acetate and lead citrate	Plastic (AGAR100)		Electron microscopy
II	NBF	f VIII – ABC technique	Paraffin	Glycerine-gelatine	Brightfield microscopy
III	NBF	Weigerts elastin or unstained for AF	Paraffin	Pertex	Brightfield microscopy or fluorescence microscopy
IV	NBF	H & E	Paraffin	Pertex	Brightfield microscopy
V	NBF	<ul style="list-style-type: none">• H & E• Massons trichrome• Sirius red• Unstained for AF	Paraffin	Pertex	<ul style="list-style-type: none">• Brightfield microscopy• Densitometry• Fluorescence microscopy

Table 2. *Preparation methods in the different studies.*

Immediately after surgery, the biopsies were placed in 4% neutral buffered formaldehyde solution (studies II – V) or in 4% glutaraldehyde in 0.1 M sodium cacodylate buffer (study I).

Before dehydration, the specimens were trimmed according to the sampling scheme discussed above.

The biopsies were then dehydrated in increasing concentrations of alcohol. The specimens in study I were also postfixed with 2% osmium tetroxide. Thereafter, the specimens were embedded in paraffin (studies II – V) or AGAR100 (study I).

The sectioning of the specimens was performed on a rotational microtome for light microscopy (Microm HM 360, Microm GmbH, Germany, studies II - V) or on an ultramicrotome for electron microscopy (Reichert OM U2 (Study I)).

After sectioning, the specimens were stained with different histochemical stains to reveal the specific structures of interest.

The histochemical staining procedures

Several histochemical staining methods were used to reveal the different tissue elements. An overview of the staining methods is given in Table 3. Recipes for the different staining methods are given in Appendix 1.

<i>Study</i>	<i>Staining</i>	<i>Detects</i>
I	Uranyl acetate and lead citrate	Membranes. Contrast enhancement (TEM).
II	f VIII – ABC technique	Coagulation factor VIII in endothelium in blood vessel walls.
III	<ul style="list-style-type: none"> • Weigerts elastin • Unstained specimens for AF 	Elastic fibres.
IV	H & E	Detects most tissue components. H & E is the standard staining method in histopathology.
V	<ul style="list-style-type: none"> • H & E • Massons trichrome • Sirius red • Unstained for AF 	See above. Epithelium, connective tissue and smooth muscle. Collagen. Elastic fibres.

Table 3. *Staining methods in the different studies.*

The histochemical staining methods are reliable, quite cheap and are more easy to use than immunohistochemistry. They are therefore preferred over immunohistochemistry whenever possible.

The immunohistochemical staining procedure

In study II, immunohistochemistry was used to reveal the endothelium in the blood vessels. After sectioning, the specimens were mounted on glass slides and prepared in the following way:

First, they were incubated with fVIII primary antibodies in room temperature for one hour (rabbit anti-human in 4% swine serum, Dako, Glostrup, Denmark). The antibodies were diluted 1:200 in phosphate buffer 0.01M, pH 7.2. Rinsing in Tris-saline buffer 0.05 M, pH 7.6 followed, and subsequently the biotin-conjugated secondary antibody (goat anti-rabbit, Dako, Glostrup, Denmark) was applied for 30 minutes. The secondary antibody was diluted 1:300 in the same buffer as above. The bound antibodies were detected by using a standard avidin-biotin-peroxidase system with 3,3'-diaminobenzidine tetrahydrochloride as chromogen. The specimens were *not* counterstained.

Stereological considerations

When the studies were planned, it was important to take into consideration the stereological rules and principles, and apply them to the studies. There are three main considerations in planning a study according to stereological practice (Leder, 1979):

1) The sampling procedure. This is described on page 27. The reason for the importance of the sampling procedure, and the randomisation process is that every part of the tissue should have equal possibility to be examined. This sampling method is called *uniform random – UR*.

2) The reference space. The reference space should be defined. It is the anatomical region where the objects of interest are located. This is an organ or a part of the tissue examined. It is defined by natural borders. Three characteristics of the reference space are needed to perform theoretically unbiased estimates. These characteristics are the following:

- The reference space must be defined.
- It must contain the tissue of interest
- It must be available

3) Sources of bias in microscopy. Bias, or systematic error, causes estimates made from samples to diverge from the true value. When bias is present, it cannot be quantified, corrected or removed. The only way to guarantee accuracy is to use tools or methods that are inherently unbiased.

Bias can be defined as stereological and nonstereological (Peterson, 1999).

Stereological bias:

- Faulty correction factors
- A sum of probe and parameter < 3
- Incorrect models or assumptions

The sum of probe and parameter must not have insufficient parameters; they must equal at least three. See Table 4.

<i>Parameter</i>	<i>Dimension</i>	<i>Structure</i>	<i>Probe</i>	<i>Dimension</i>	<i>Sum of Dimensions</i>
Volume	3	Volume	Point	0	3
Area	2	Surface	Line	1	3
Length	1	Linear	Plane	2	3
Number	0	Cardinality	Disector	3	3

Table 4. The dimensions and sum of dimensions for different parameters and structures.

Nonstereological bias:

- Incomplete / bad staining
- Ascertainment bias; systematic error in sampling individuals from a target population
- Improper calibration or observer bias
- Incorrect mathematics

Stereological considerations in the different studies

In **study I**, a hierarchical sampling scheme was used (Study I, Fig. 1). From one block, three grids with one section each were prepared. From each section, micrographs were obtained from three areas. From each area, finally, ten collagen fibrils were measured. This means, that from each block 90 fibres were measured. The parameter measured was the minimum diameter (D_{\min}) in the fibril. By using D_{\min} , the actual fibril diameter was always measured, even if the fibril was not cut exactly perpendicular (Fig. 10).

In **study II**, biopsies from the vestibulum vaginae were immunostained to reveal blood vessel walls (endothelium). From each biopsy, six consecutive sections were quantified by random selection of one field per section. A cycloid grid according to the method described in Baddeley et al. (1986) was used.

In **study III**, The detection of elastic fibres was compared between the new autofluorescence method and specimens stained with Weigerts elastin stain. Two consecutive specimens from each biopsy were sectioned. One was stained with Weigerts elastin stain; the other left unstained but covered with a coverslip. The elastic fibres were measured as average area fraction from three areas in the same specimen with the image area as reference area.

In **study IV**, the epithelial structure was measured. From each paraffin block, the first usable section was taken. The following five sections (average sum of thickness = $5 * 5 \mu\text{m}$; $25 \mu\text{m}$) were discarded. The next section was taken, the following five discarded, and then the last section was taken (Fig. 11). This gives a depth of about $75 \mu\text{m}$ in the tissue.

In **Study V**, The same procedures as mentioned above were used for elastic fibres and epithelium. For the elastic fibres, only the autofluorescence method was used in this study. The sectioning strategy is discussed in Fig. 12. The amount of collagen was determined by staining the specimens with Sirius red and measuring the intensity of transmitted light from a stabilised light table through them. The amount of smooth muscle was measured by the use of a virtual line grid placed over the image of the Massons trichrome-stained specimen. The area fraction of smooth muscle fibres was calculated by counting the line intercepts.

Image analysis

An overview of the image analysis setup is given in fig. 13. An overview of the image analysis process in general is given in fig. 14. In general, the image from the microscope is taken into the computer in 8 bit RGB-mode via the framegrabber. This process, ending with the image stored in the primary memory of the computer, is called *image capturing*. The image is then split into its three greyscale components, and the most suitable of the component images (usually but not always the green component) is chosen for further processing.

Image enhancement

The next step in the image analysis process is often enhancement of the image (Kalra et al., 2004), for example noise reduction (Techavipoo et al., 2004), contrast expansion and correction of uneven lighting. This is done by built-in correction algorithms (Landmann and Marbet, 2004).

Image segmentation and thresholding

Segmentation of an image means to reduce the image information to the information of interest (Waarsing et al., 2004). The process is used to divide the image into regions that contain the structural units of interest (Zhang and Chen, 2004). The segmentation process is often described as separation of the background from the foreground, in analogy with the visual process.

Thresholding is done after defining a range of brightness values in the original image. As mentioned above, the images are stored as three 8-bit greyscale component images. Each image then comprises $2^8 = 256$ greyscale values. The threshold is set so that all pixels with a greyscale above the threshold will be selected for further processing. Usually, the thresholding process generates a binary image (only consisting of black and white pixels) where the structures of interest are white and the background is black.

Image measurements

The measurement step can be considered the real analysis process. The previous steps were different image processing steps to make the resulting image suitable for the final measurements. In contrast to the image processing steps, the measurements performed attempted to find the descriptive parameters, usually numeric, that represent the information contained in the image.

There are many things a microscopist can want to measure in images; volumes, area fractions, numbers etc. All this can be done, but regarding the process of *image measurement* that is performed by the computer on the single image or on the ROI, the measurements that can be performed can be classified into four categories:

- Brightness
- Location
- Size
- Shape

Image analysis strategies in the different studies

This text focuses on the image processing operations, image enhancement, filtering and segmentation etc. and leaves out the image capturing, which is similar in most of the studies. In study V, however, it is included for the collagen intensitometry, since it is done in a different way here. See Appendix 2 for flowcharts over the computer programs.

In **study I**, the first step consisted of median filtering to remove noise in the image. Thereafter the image was thresholded and area measurements were performed in the binary image. The fibres to be measured were selected manually by pointing at the fibre.

In **study II**, after capturing, the image underwent a shading operation to remove uneven illumination. The blue component image, with the most suitable greyscale range was subsequently stretch filtered to increase contrast. On the resulting image, two GOP[®]-operations were performed to further reveal the image information. The first was an orientation operation, to estimate the orientation of the blood vessel structures. The second operation was a phase operation that detects the pixel positions in the edge- and line-like structures. A virtual cycloid grid was then superimposed on the resulting image. The grid was taken from a database library. A Boolean *and*-operation excluded everything except the intercept points from the image, and the number of points could thereafter easily be counted by the computer program and saved to a file.

In **study III**, two different methods for visualisation of elastic fibres were used, and therefore two different image analysis strategies were employed.

For the specimens stained with Weigerts elastin stain the green component image was chosen for image operations. For the unstained specimens, the red component image was chosen.

The following image operations were the same for the both types of specimens. First, absolute stretch filtering was performed with manual control of the *high* and *low* values of the filter. A contextual line-operation outlined the lines, which subsequently were thresholded manually. Finally, the lines were measured as area fraction of elastic fibres with the image area as reference area.

In **study IV**, a profile of the epithelial structure was created in two steps. First, the basal layer was thresholded and saved as a binary image. This was a quite easy operation in most cases, since the basal cell layer normally is darker than the rest of the epithelium. Then, the whole epithelial structure was thresholded. This operation often included many subepithelial structures in the resulting image. By a Boolean *exor*-operation the epithelial profile was outlined.

If DPs are present in the epithelium, the length parameters are measured. If no DPs are present, only the distance from the basal layer to the surface (BLS) is measured.

In **study V**, the computer programs and the methods discussed above were employed. In addition, *collagen fibres* were measured by intensitometry, i.e. detection of the optical density of collagen fibres stained with Sirius red. The light table was allowed to stabilize for ½ h before measuring. The camera settings were carefully adjusted and remained the same throughout all measurements. The specimen was put on the light table, and an image sent to the computer. On every image, calibration was performed to set the white level. The profile of the specimen was then thresholded and a binary image created. The binary image of the specimen was superimposed on the original image, leaving only the specimen against a black background.

The results are given as a ratio between the two analysed phases, in this case collagen fibres and background. As reference area, the area of the entire specimen was used. The results of the measurements were in the range of 40 to 50 percent among the ten subjects, indicating a low variability (Fig. 7 Study V).

The first step in the program for *smooth muscle* detection was to convert the colour space from RGB to IHS. A stretch filtering operation was performed on the hue component to expand its greyscale range. This was followed by a contextual phase-operation, which estimated the positions of the pixels in the line- and edge-like structures of the smooth muscle fibres. The resulting image from the phase-operation was thresholded, and the binary image produced contained the profiles of the smooth muscle fibres. Subsequently, a virtual line grid was superimposed on the image of the fibres, and by a Boolean *and*-operation only lines hitting the fibre profiles were left. The number of profiles was thereafter automatically counted.

Statistical interpretation of data

I: The data from TEM were analysed according to analysis of variance (ANOVA), using a hierarchical design, according to a model described in a previous study (Olenius et al., 1991).

II: The blood vessel volume fractions were analysed with Mann-Whitneys U-test for small samples.

III: The Wilcoxon matched-pair test was used to analyse the area fractions of the elastic fibres.

IV: For the correlation analysis of the image analysis program vs. manual measurements, Pearson's correlation test was used.

For the consistency analysis of the image analysis program vs. manual measurements Mann-Whitney's U-test was used.

V: Basic statistic calculations were used to present data from the measurement results. Since only one group of healthy subjects was investigated, no statistical comparison was performed.

Results

Results regarding the developed methods: Study II, III & IV

A computer program for contextual detection and stereological measurement of immunostained blood vessels was developed. Despite the complexity of the tissue morphology, the measurement procedure was found stable and error-free. The procedure was easy to learn and use, without demands on expert computer skills. Typically, all calculations depended on some manual interaction, but without being too much of a repetitive routine, nor time-consuming or difficult (II).

A computerised method for detection of elastic fibres, stained either with Weigerts elastin stain or unstained and detected by their autofluorescence was developed. The elastic fibres detected by autofluorescence were easily distinguished and could readily be quantified. Virtually no manual correction or segmentation of the computer images was needed before the morphometric analyses. Consecutive sections stained with Weigerts elastin stain produced a similar pattern of the elastic fibres, in this case stained blue-black (Fig. 2, Study III). For these specimens, both stretch filtering to enhance the contrast of the fibres (Fig. 3, Study III) and manual removal of background was required in most cases, since nuclei belonging to various cells in the connective tissue were stained greyish blue and the collagen in the connective tissue also showed some greyish staining. This manual removal of background consisted of painting a dot on the structure that should be removed. After the painting was finished, a touch operation compared the layer with the painted dots with the image and by the use of Boolean operations, removed the items, i.e. cell nuclei and resets the background colour to black (III).

A semi-automatic image analysis program intended for advanced evaluation of the epithelial profile was developed. The size of the program was 13 kB. The program was designed to allow manual interactions 6 times at critical points.

The reasons for allowing manual interactions were to assure that the program could run independently of the staining quality of the specimen and to set checkpoints where the operator was able to judge and influence the outcome of the program steps and the quality of the produced intermediate images.

The image analysis process, from insertion of the specimen in the microscope to achieving the measurement results, took about 7 min. The corresponding time of the same procedure done manually with pencil and ruler on a paper copy of the image was about 45 min. The program was designed to be self-instructive and not demand an operator with special computer skills.

The image analysis program was developed using a Sun Sparc20 Unix computer and the MicroGOP 2000s software. The programming language was a C-like interpreting language. This program can also run on other computer platforms such as X86 and Microsoft Windows™ platforms with the MicroGOP 2000s software and optional hardware.

The image analysis program was primarily designed for haematoxylin and eosin stained specimens. It could, however, also detect brown stains, i.e. cytokeratin immunohistochemistry using a detection system of peroxidase-conjugated secondary antibodies (IV).

Epithelium: Study IV & V

Instead of only measuring the epithelial thickness, which would be a biased measurement, a computer program was developed that took the entire structure, including connective tissue papillae, into consideration. The epithelial structure was measured with its four defined structural parameters; BLS, DPS, DPW and DPD (Fig 4, Study IV). In study IV, the computer program was validated. Therefore, measurements from the same images of epithelial tissue were performed both by hand, with pencil and ruler, and by the computer. The results obtained by the computer program correlated well with the manual measurements (Fig. 10, Study IV). All four measurement parameters were significant at $p < 0.05$. For BLS, the r-value was 0.995, for DPS 0.980, for DPW 0.988 and for DPD it was 0.996.

The results of the measurements from the structural parameters should then be presented in a distinct and simple way. A graphic presentation of the measurements was made by inserting the results in so-called star graphs (Fig. 11, Study IV). These graphs plot the parameters, each on its own axis, as dots connected with lines. For each defined epithelial type, a specific area was then produced in the graph.

Epithelium without DPs, however, shows no area in the star graph, since only the distance from the bottom of the basal layer to the epithelial surface is measured, and all the other parameters are set to zero (IV).

The epithelial structure showed substantial differences among the subjects. In four of them, subjects 1, 6, 7 and 8, no connective tissue papillae were found at all, and thus only the distance from the epithelial basal layer to the surface (BLS) could be measured. Among the other parameters measured in the subjects that had dermal papillae, the one showing the greatest variance was the distance from the dermal papilla to the surface (DPS). The parameter showing the smallest variance was the dermal papilla width (DPW). The mean and median distances for all parameters among the ten specimens were calculated (Table 3, Study V). To give an orientation to the individual values, the four measured parameters for all ten specimens were plotted as star graphs (Fig. 5, Study V) (V).

Collagen: Study I & V

The collagen fibril diameter was analysed with transmission electron microscopy. The control group showed a significantly smaller fibril diameter, expressed as D_{\min} , than the SUI group. The median diameter was 58 nm in the control group compared to median 76 nm in the SUI group, $p = 0.005$ (Fig. 2, Study I) (I).

The collagen content in the light microscopic specimens was analysed by intensitometry. This method gives the result as a ratio between the two analysed phases, in this case collagen fibres and background. The results of the measurements were in the range of 40 to 50 percent among the ten subjects, indicating a low variability (Fig. 7 Study V) (V).

Vasculature: Study II

Sections from the vestibulum vaginae from ten patients suffering from vestibulitis and ten healthy subjects were used for the morphometrical measurements. An abundant vascularisation of small-calibre vessels, mainly consisting of capillaries, was present in all tissue sections in both groups. The results of the microvascular quantification in the vestibular mucosa were almost identical in the two groups. In the patients, the blood vessel area per volume was $78.1 \pm 13.2 \text{ mm}^2/\text{mm}^3$ (mean value \pm SEM). In the controls, it was $76.5 \pm 8.1 \text{ mm}^2/\text{mm}^3$.

A detailed statistical analysis revealed that the major part of the variance could be attributed to between-subject rather than within-subject variation. This indicates that the preparation routine of the described procedure is stable and its counting method reliable.

Elastic fibres: Study III & V

In study III, the autofluorescent method was compared to one of the most widely used staining methods for elastic fibres, Weigerts elastin stain.

Using the autofluorescent method, ultraviolet light in the range of 450 – 500 nm induced a distinct fluorescence from the elastic fibres (Fig. 1, Study III). The signal was very high compared to the background and significantly higher than other autofluorescent elements in the tissue, i.e. collagen fibres and red blood cells. This made it very easy to segment the image and remove the background from the elastic fibre profiles.

When the area fraction of the elastic fibres was measured, the elastic fibres were calculated as area fraction with the rest of the image (connective tissue) as reference area (Table 1 Study III). Quantification using the autofluorescence method showed that $4.7 \pm 0.8\%$ (mean, standard error of mean) of the total area consisted of elastin fibres. The Weigert elastin staining method also gave a value of $4.7 \pm 0.8\%$. The Wilcoxon matched pair test showed no significant difference between the measurements performed with the two staining procedures (III).

The elastic fibres constituting the elastic membrane were measured as area fraction with the rest of the image as reference area. When the unstained specimens were viewed in fluorescent light in the range of 450 – 500 nm, a distinct fluorescence was induced from the elastic fibres. The mean value of the fibre area fraction was fairly consistent between 0.2 and 2.7%, but the variance was high in most of the specimens (Fig. 6 Study V) (V).

Smooth muscle: Study V

To calculate the amount of smooth muscle fibres, a virtual point grid was placed over the images. The fibres were calculated as area fraction from two images in the same specimen. The smooth musculature was also highly variable, (Fig. 8 Study V). Two specimens, numbers 6 and 8, showed almost no smooth muscle fibres, while subject 7 showed the highest amount of smooth muscle fibres.

Discussion

Discussion of development of methods

Some of the developed methods are based on stereological methodology. It is impossible to discuss the newly developed methods without including information and discussion about established stereological methodology.

Participants

Effort was made to select a homogenous group of women regarding age and gynaecological status. Overweight women ($BMI > 30 \text{ kg/m}^2$) were excluded. Women with systemic disorders or using medications were also excluded. Another exclusion criterion was malignant conditions, since this could affect the histopathological results.

In study IV, the exclusion criteria were not so strict, since the main purpose of this study was to evaluate the measurement method against a number of different types of epithelial specimens. Here, the structure of the epithelium was the important factor, not the age or condition of the subject to whom it belonged. However, none of the participants of this study suffered from malignant conditions.

Sampling and stereology

Since this thesis is based entirely on biopsy specimens from the vaginal wall or vestibulum vaginae in living women, it is impossible to define the reference space (Hunziker and Cruz-Orive, 1986) as “the vagina” or “the connective tissue”, “the epithelium” etc.

There are in this case two main reasons why the reference space could not be defined: First, the tissue (epithelium, connective tissue and musculature) shows ill-defined marginal limits. The tissue blends into adjacent structures, such as the cervix cranially and perineum caudally. The second reason is that the studies were performed on living women, which allowed only small biopsies to be taken.

In this case, *reference areas* and *stereological ratios* (Wulfsohn et al., 2004; Cruz-Orive and Weibel, 1981) can be used instead. In virtually all studies carried out on living subjects, where biopsies are obtained, this is the only method available.

Even if the reference space cannot be defined, the first thing to be decided is the fundamental sampling unit (FSU). This can be the whole organism (human body), the organ, tissue or cell. In the present studies, the FSU is in most cases the tissue area. For example, the elastic fibres are measured as an area fraction, with the image area as reference area.

When reference space and –area are discussed, a very important consideration is the *reference trap* (Braendgaard and Gundersen, 1986). This trap is especially easy to fall into if the results rely on ratio estimations. If the tissue shrinkage is different in the two groups that are to be compared, the results can be completely wrong unless this is taken into account (Haug et al., 1984).

Except in studies I and II, the studies included in this thesis did not compare two groups. In all studies every biopsy was taken in a uniform way by an experienced gynaecologist. The women did not differ much in age. Fixation and histological preparation was also performed uniformly according to standard protocols. All the histotechnical work, as well as histopathological examination and morphometrical work was performed in a GLP facility. The studies could not be conducted according to GLP guidelines (Baak, 2002; Brunetti, 2002), but were performed to a similar standard.

Histology and staining technology

Instead of always using immunohistochemistry for the detection of different tissue components, classical histochemistry was used when possible (Horobin, 2002; Lyon et al., 1994). Histochemistry is cheaper, less time-consuming, often easier to apply and also often more accurate when it comes to the detection of large tissue components, such as collagen and smooth muscle. However, there are many occasions where immunohistochemistry is the only solution. In study II, it was used to detect blood vessel walls. For this application, it is superior to any classical histochemical stain for specific structures.

The collagen measurement performed in *study V* was not performed with stereological methods. Instead, intensitometry was used (Sutoo et al., 2002). This technique is sometimes also referred to as microphotometry or densi-

tometry (James et al., 1986). In this technique, the optical density of objects is measured, i.e. the amount of light passing through a tissue (Ma et al., 2001). The tissue measured must of course be stained in a proper way to give it contrast. To stain the collagen tissue in study V, the anionic dye Sirius red F3BA was used (James et al., 1990). Collagen fibres are stained intensely red when stained with an aqueous Sirius red solution saturated with picric acid. This is also referred to as the picosirius reaction. A possible mechanism for this reaction is that the sulphonic acid group of SR interacts at a low pH with the free basic side-chains of the amino acids lysine, hydroxylysine and arginine in the collagen fibre. The picric acid prevents most other structures than collagen to be stained by SR. According to a theory, SR binds to the collagen molecule in such a way that the long axes of both the collagen and SR molecules are parallel. This could be an explanation for the fact that the normally weak birefringence of collagen is greatly enhanced after the picosirius reaction. The picosirius reaction is very specific, and also very sensitive, for demonstration of collagen (Lopez-De Leon and Rojkind, 1985). It is also very stable, and seems not to deteriorate with time.

Image analysis

Computer-assisted image analysis is a relatively common technique (Bryan, 2003; Eils. and Athale, 2003), which has been used in many biological studies since the development of microcomputers (Arenson et al., 1990; du Boulay, 2000; Mixdorf and Goldsworthy, 1996). This technique cannot by itself give an assessment about volume and area relations. Image analysis is best suited to quantify immunohistological staining and similar preparations. To quantify volumes and areas in histopathological specimens, stereology should be used in the first place. Stereological methods are often described as simple, despite the mathematics involved (Gundersen et al. 1988). They are also described as less technically demanding than image analysis. Often, image analysis methods are described as considerably more complicated, demanding a higher technical skill and more equipment than stereology. Also, they can in many cases be slower and more time-consuming than the stereological methods (Gundersen et al., 1981).

To make a computer-assisted morphometrical method useful, the following criteria must therefore be fulfilled:

- A simple sampling methodology based on stereological methods
- A clear and well-arranged development environment for the creation of the morphometrical applications
- A user-friendly programming language
- Implementation of stereological methodology directly in the image analysis program application

- The resulting morphometrical applications must be user-friendly and must be able to run even by operators lacking expert computer skills.
- The resulting morphometrical applications must be faster than the similar stereological methods.
- The resulting morphometrical applications must be as accurate as the similar stereological methods.

One of the major problems regarding computer-assisted image analysis has been the difficulty of segmenting biological images in order to extract interesting information (Saatci and Tavsanoğlu, 2003). However, using the contextual methods offered by the GOP[®]-technology the segmentation process has been greatly facilitated (Context Vision AB 1987).

During the development of the morphometrical applications (except study I) included in this thesis, a Sun SparcStation 20 Unix computer platform was used. The image analysis software used for all the applications (except study I) was MicroGOP 2000S. Optional hardware used together with the computer, consisted of a MIP processor board for the GOP image operations and also for some other filtering operations. The programming language was a C-like interpreting language.

For study I, the Kontron IBAS image analysis system was used.

Discussion of the findings in the different experimental setups

The results from the measurements of epithelium show a considerable variability. This variability seems to be a variation among individuals, even in the same age. Some women have a rather thin epithelial lining without DPs, while others have a considerably thicker epithelium with numerous DPs. It is obvious that oestrogen therapy makes the epithelium thicker, with more cell layers. It seems, however, that the variability in epithelial structure is large even without hormonal therapy. With the measurement strategy described in this thesis, it is easier to describe the structure of the epithelium, instead of just measuring epithelial thickness, a measurement that can be performed in a number of ways (Benedet et al., 1992; Albert et al., 1992; Wilkinson EJ, 1992; Moragas et al. 1993; Sanders et al. 1998). This new method is standardised, which is a great advantage over previous methods. The measurement results can be used to measure and monitor the height of the epithelium, as well as the number, height and width of the dermal papillae. This is of great importance, not only for histopathological studies, but also to inves-

tigate epithelial changes under hormonal therapy (Whitmore and Levine, 1998; Sator et al., 2001). It will also be useful for studies of skin grafting or breast reconstruction using expanded skin (Olenius and Johansson, 1995).

The results from the collagen morphometry show that the collagen fibrils in premenopausal women suffering from SUI have a significantly increased diameter. The results suggest that the tissue might be less flexible (Roughley, 1992). A stiff urethra may not close properly, and can result in urinary incontinence (Petros and Ulmsten, 1993). For this reason, the method for measurement of collagen diameter has generated interest among scientists in this field.

To measure the diameter of collagen fibrils at the ultrastructural level is one approach to assessing the connective tissue. Another approach, at a lower magnification, is to perform intensitometry on specimens stained with the collagen specific and α -sensitive stain Sirius red (James et al., 1990; James et al., 1986; Marotta and Martino, 1985). The reason for choosing intensitometry instead of, for example, point counting, is that most of the specimen consists almost entirely of connective tissue, and point counting would yield a nearly 100% fraction of collagen. Intensitometry is often used to detect immunohistochemical staining intensities (Danielsson et al., 2003). In clinical studies, the amount of collagen in a tissue can be of importance, for example in the assessment of urinary incontinence or in skin expansion studies (Falconer et al., 1998; Olenius et al., 1995).

The stereological method used for the blood vessel measurements employs the calculation for estimation of surface area from vertical sections (Baddeley et al., 1986). The blood vessels are measured as surface area, in mm^2 with the connective tissue in the measurement frame as reference area. The formula used in this calculation makes it possible to give the reference space as volume, in mm^3 . The results are therefore presented as blood vessel area fraction in mm^2 per connective tissue volume in mm^3 . An important prerequisite for this method is that the section is *vertical*. A vertical section is defined as a plane section perpendicular to a given horizontal plane. The vaginal wall with its epithelial lining is therefore a vertical section, and can be used for surface area measurements if care is taken to cut the sections as vertical as possible.

This method was used to measure the amount of blood vessels in a study of vulvar vestibulitis. However, there are many cases in which vasculature is of interest. In studies of menorrhagia, it can be a helpful tool (Mints et al., 2002) and in tumour diagnosis it can be used to assess neovascularisation (Edovitsky et al., 2004). When studies are designed with this method, it is important to bear in mind that the sections must be vertical.

The elastic fibres are difficult to measure by biochemical methods (Gosline and Rosenbloom, 1984). Elastin is not readily soluble. Instead, elastic fibres can be detected by a number of histochemical staining methods. One of the most commonly used methods is Weigerts resorcin-fuchsin stain, in common histopathology referred to as Weigerts elastin stain (Weigert, 1898). In *study III*, a novel, simple and interesting method to detect elastic fibres in histological specimens is presented. The discovery leading to this method is that the elastic fibres show a very bright autofluorescence when viewed in the fluorescence microscope. Since no staining whatsoever is needed, and the light emitted from the fibres is sufficiently bright, this is well suited for morphometrical measurements.

In study III, morphometry using the autofluorescence method was compared to morphometry using Weigerts elastin stain to detect the elastic fibres. The results were the same for both methods. However, the autofluorescence method was much faster and much less manual interaction was required.

The results from study III differ considerably from the results from study V. In study V, the amount of elastic fibres is much less than in study III. This is likely due to the different biopsy sites in the two studies. It has previously been observed that specimens taken from the introitus contain a large amount of elastic fibres (Blomgren, unpublished results). Obviously, the intra-individual variance in elastic fibres in the vaginal wall is considerable. Depending on the region, the connective tissue in the vaginal wall can contain from occasional fibres to a thick layer. This layer can be so thick that it actually is more than a membrane (Fig. 15).

The measurements of the smooth muscle tissue were performed by counting line intercepts. The computer program developed for this measurements was similar to the program for blood vessel measurements. It also used a virtual grid, but instead of cycloids, the program for measurement of smooth muscle used a line grid.

The results showed a considerably variability in smooth muscle tissue in the vaginal wall. The subject with the highest amount of smooth muscle fibres had a ratio of 0.31% smooth muscle fibres per surface area. The subject showing the lowest amount had below 0.01% smooth muscle fibres per surface area. This extremely high variability was also seen when the specimens were examined in the microscope. The preparation of the tissue, from the surgical excision of the biopsy to the histotechnical procedures, was carried out carefully and uniformly. The reason for this great variability is unclear, but it is unlikely that it is caused by a preparation artefact. It might instead be a sign of early atrophy (Boreham et al., 2002).

Future perspectives

Morphometric studies based on stereology and image analysis will have great impact and considerable value regarding quantification of tissue components. Computer-assisted technique facilitates the often rather complicated stereological measurements. A great interest has been shown in clinical science, for example gynaecological science. Also, in preclinical science where animal models are used, these techniques can be applied to reveal pathological changes or other tissue-associated data. One interesting example is phenotyping of transgenic mouse models.

An increasing demand for morphometric analysis has also been noted in toxicological studies in pharmacological science. Regulatory authorities will more commonly demand objective methods for quantification in toxicological pathology. Considering the demand on “high throughput” in the pharmaceutical industry today, these methods will suit the task well.

Another interesting field is the use of computer-assisted image analysis for automated detection of histopathological sections. These methods are often based on advanced statistical algorithms or neural networks. System development for tumour diagnosis has started, and in the future, this method may aid the pathologist in the diagnostic process. However, much work has to be done before these systems can replace the pathologist in making the primary tumour diagnosis.

Conclusion

The following are the main methodological conclusions of this work:

Study III: A method for computer-assisted contextual detection of the auto-fluorescence from elastic fibres was compared with similar analysis of elastic fibres stained with Weigerts elastin stain and examined in an ordinary light microscope. No difference regarding the measurement results was seen between the two methods.

Study IV: The developed computer-assisted method for measurement of epithelial structure was found to be a reliable tool. Since length, size and number of the papillae may vary with different pathological conditions, age and hormonal status, this method is considered a possible tool in the diagnosis of such conditions.

Study V: This study was designed as a summary of the previously developed morphometrical methods, with two additional methods. The different tissue components (epithelium, collagen, elastin and smooth muscle tissue) were easily detected by the computer-assisted morphometrical methods.

The following were the clinical findings of this work:

Study I: Ultrastructural measurements of collagen fibrils revealed larger diameter of the fibrils in fertile women suffering from stress urinary incontinence than the fibril diameter in the control group.

Study II: A computerised method for contextual detection followed by stereological measurement of immunostained blood vessels was developed. Using this method, no differences in blood vessel area could be detected in patients suffering from vestibulitis compared to healthy women.

The results from the present studies show that correctly applied morphometry is of great importance in performing a survey of the microscopical anatomy in the vaginal wall, as well as in performing quantitative analysis of its tissue components. This methodology is clearly as useful for all quantitative analyses in histology.

It is very important that the developed methods are simple and user-friendly. They should also be faster than the original stereological methods, a goal not always achieved by computer-assisted methods (Gundersen et al., 1981).

Figures

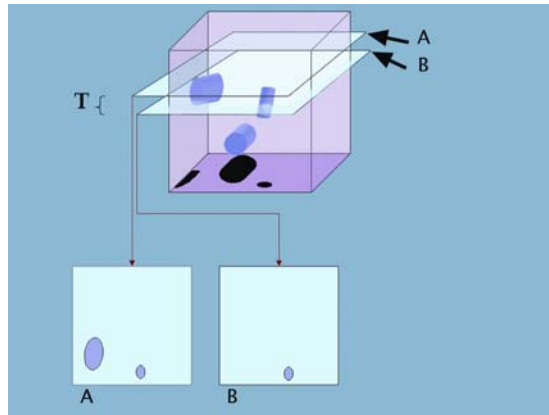


Figure 1. The disector principle. Two sections (planes) are placed in a volume a known distance apart (T). Objects in the volume will be seen as profiles on the slices. The big object to the right is seen on slice S1 but not on S2 and are therefore counted. The smaller object to the left is seen on both slices. It is not counted yet. It will be counted on the slice before it disappears.

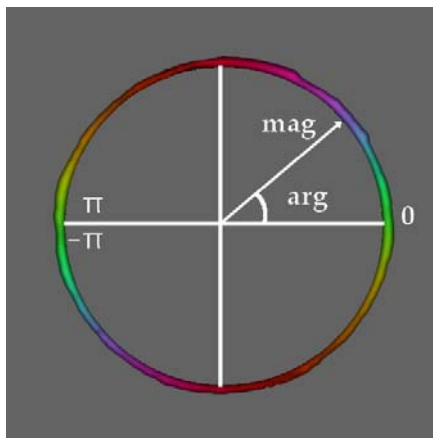


Figure 2. The GOP[®] circle. A special colour scheme is used for the angle, or argument (arg), of the vector. The length of the vector, the magnitude (mag), depends on the strength of the feature analysed.

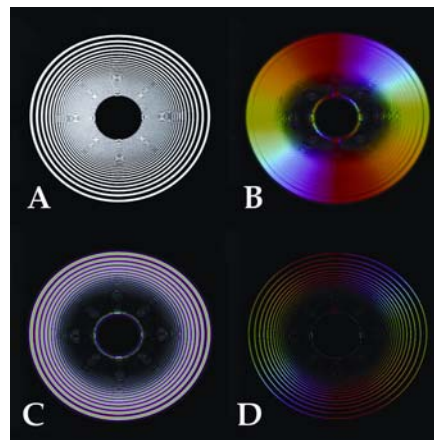


Figure 3. The test image “Ploop” (a) consisting of concentric circles, is used to demonstrate some GOP operations. In (b) the Orient operation is shown, in (c) the phase operation and in (d) the line operation.

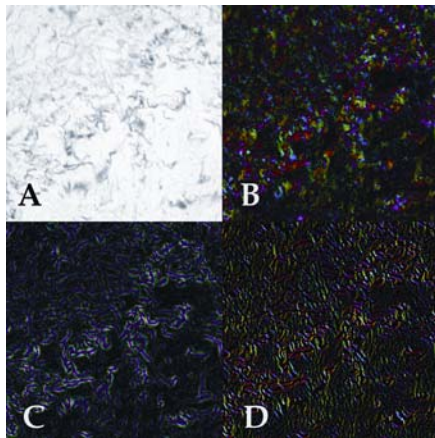


Figure 4. (a). The same operations as in fig. 3 are performed on a specimen consisting of elastic fibres (black and white image). In (b) the Orient operation is shown, in (c) the phase operation and in (d) the line operation.

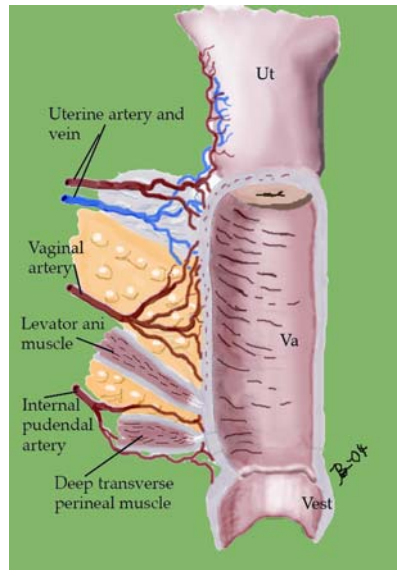


Figure 5. The vaginal anatomy. Muscles and blood supply. Ut: Uterus. Va: Vagina. Vest: Vestibulum.

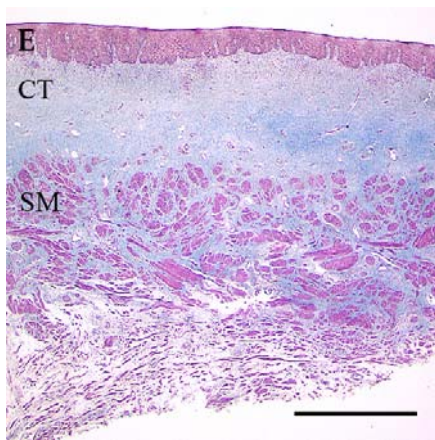


Figure 6. The histological structure of the vaginal wall. The three main tissue components are clearly visible. E: epithelium, CT: connective tissue, SM: smooth muscle. Masson's trichrome stain. Scale bar = 2000µm.

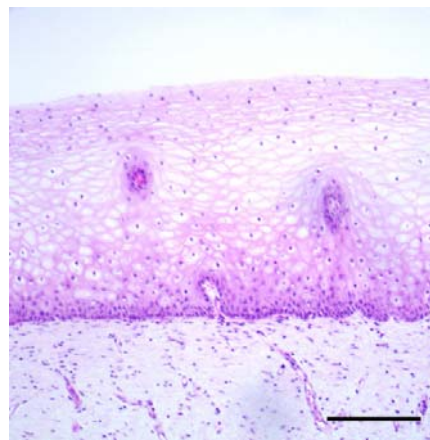


Figure 7. Epithelium from the upper anterior part of the vaginal wall. Note the pale, bulging cells with small pycnotic nuclei. This is typical for glycogen-laden epithelial cells. Hematoxylin and eosin. Scale bar = 100µm.

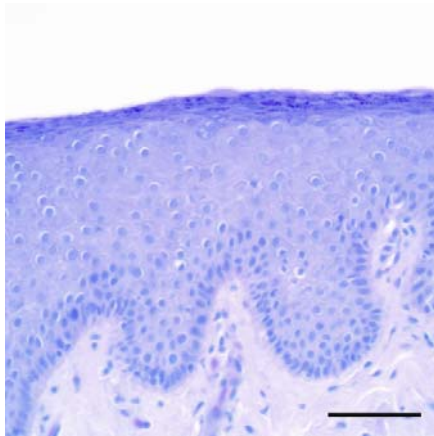


Figure 8. Epithelium from the lower anterior part of the vaginal wall. Keratohyaline granulae are visible in the upper layer of the epithelium. Hematoxylin and eosin. Scale bar = 50 μ m.

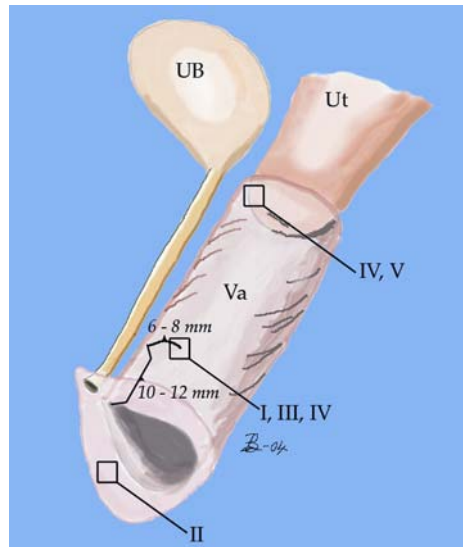


Figure 9. The biopsy sampling sites in the different studies. In studies I, III and IV, the biopsies were taken 10 – 12 mm from the vaginal orifice and 6-8 mm lateral from the urethra. In study II, the biopsies were taken from the vestibule, near the right Bartholin gland. In studies IV and V, the biopsies were taken from the anterior vaginal wall near the cervix. These biopsies were taken transvaginally during hysterectomy. Ub: Urinary bladder. Ut: Uterus. Va: Vagina.

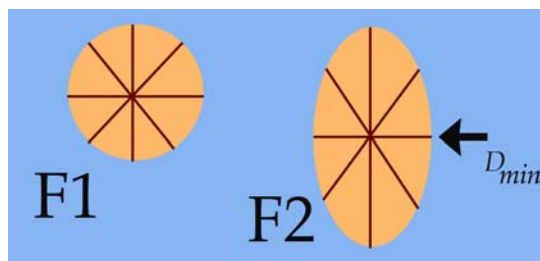


Figure 10. F1 shows a perfectly perpendicular cut fibre, where all diameters are the same. F2 shows an obliquely cut fibre. The minimum diameter (D_{min}) is the same as the diameter if the fibre was perfectly perpendicular cut.

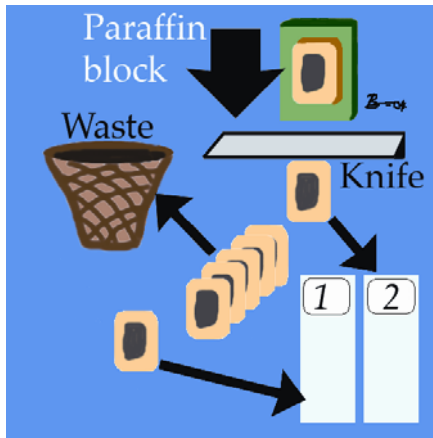


Figure 11. The sectioning strategy in study IV. The first good section is placed on a glass slide. The following five sections are discarded. The next section is placed on another glass slide.

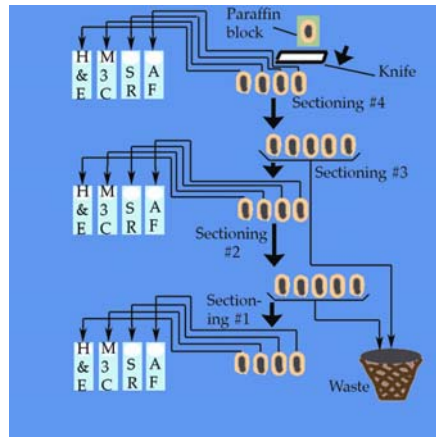


Figure 12. The sectioning strategy in study V. The first four good sections are placed on slides. The first for staining with H & E, the second with M3C, the third with SR and the fourth is left unstained for autofluorescence examination (sectioning #1). The five following sections are discarded (sectioning #2). The following four sections (sectioning #3) are placed on slides in the same way as in sectioning #1. The following five sections are discarded (Sectioning #4). The last four sections are placed on slides in the same way as in sectioning #1 and #3.

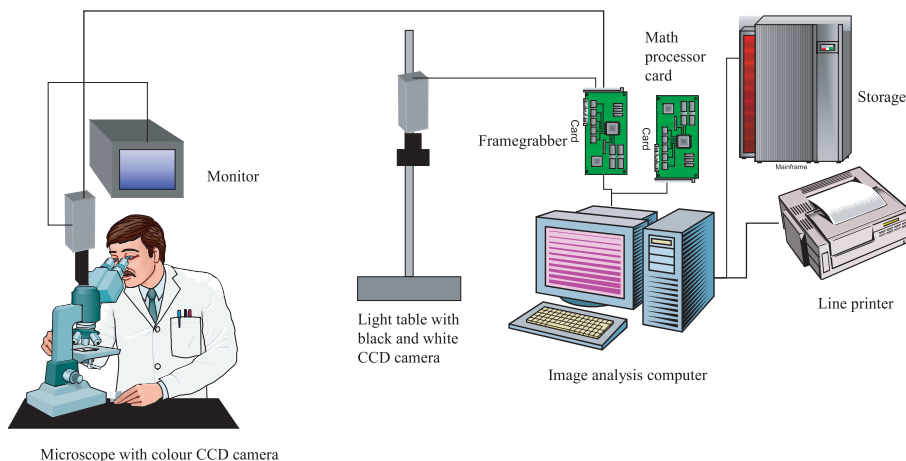


Figure 13. A schematic drawing of the image analysis setup.

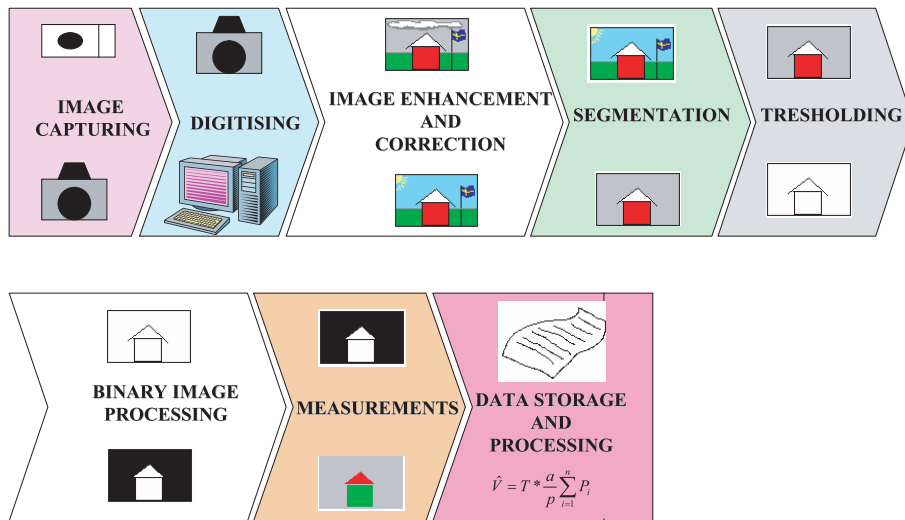


Figure 14. A schematic drawing of the image analysis process. In the first step, the *image capturing*, the image is taken by the camera and transferred to the computer. It is still an analogue signal. In the *digitising* step, the image is converted from analogue to digital by the frame grabber. It can now be stored in the computer. With *image enhancement and correction*, defects such as uneven lighting are corrected. Here the cloudy sky has been replaced by sunshine. The *segmentation* process divides the image in structures of interest (here: the house) and background (here: the ground, sky and flagpole). The *thresholding* eliminates pixels under a certain grey value, and replaces them with black. The result is a binary image. *Binary image processing* consists of the final adjustments before measurements. The Boolean operations are performed here. The house is converted to a white rectangle and triangle on a black background by a Boolean *Not*-operation. In the *measurement* step, different features such as area, perimeter, length etc. are measured. Here, the areas of the rectangle and triangle are measured. Finally, the measurement data are stored for further processing.

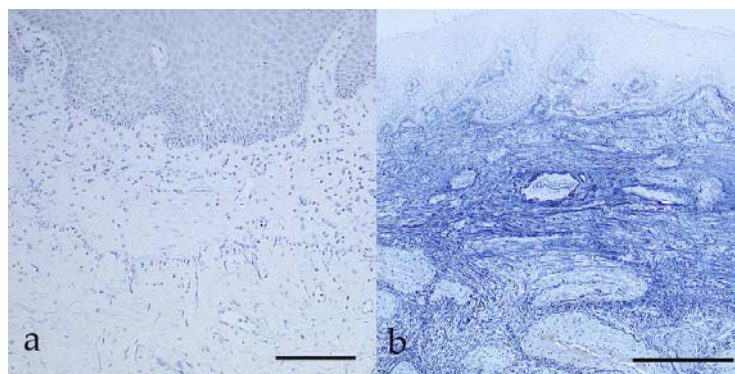


Figure 15. Two specimens stained with Weigerts elastin stain are compared. Specimen (a) is taken from the site used in studies I and III. Specimen (b) is taken from the vestibule. Note the huge amount of elastic fibres in (b) and the few fibres in the elastic membrane in (a). Weigerts elastin stain. Scale bars (a) = 200 μm , (b) = 500 μm .

Acknowledgements

There are many people who have shown interest and taken time to help me during my work. I wish to thank everyone, but I am especially indebted to:

The late professor **Ulf Ulmsten**, my first supervisor. I am grateful to him for introducing me to the interesting field of gynaecological morphology, and for acting as a guarantor for my doctoral education.

Professor **Godfried Roomans**, my supervisor, for many interesting discussions about morphometry, histology and electron microscopy. For constructive criticism of the framework of the thesis. And especially for taking care of me after Ulf Ulmstens decease.

Associate professor **Marita Hilliges**, associate supervisor, for invaluable help with the manuscripts, for good viewpoints on morphometry and stereology and for presenting me the idea of a computer program for epithelial measurement. I thought that program would be finished within a “coffee-break”!

Associate professor **Christian Falconer**, associate supervisor, for much fruitful scientific collaboration, for taking me as a member in the scientific team when you worked with your thesis, and introducing me to the interesting field of collagen ultrastructure. I am also very grateful for all the skilfully sampled biopsies you have provided me with. I think no one understands the importance of randomisation like you!

Professor **Bente Pakkenberg**, for taking your time with my work and giving good criticism and tips about stereological methodology.

Dr. **Nina Bohm-Starke**, co-author, for great collaboration with blood vessel studies, and also with epithelial structure studies.

Dr. **Ulrika Johannesson**, co-author, for kind support and cooperation.

Kenneth Olsson and **Björn Hamberg**, skilful technicians and embalmers, for helping me with trimming and fixation of some of the biopsies, and also for being such good pals.

Dr. **Ivar Paulson**, for early morning discussions about life, universe and everything. This sometimes includes discussions about morphometry and my thesis.

Dr. **Tom Holland**, for kind help with statistical problems, and for revising my English. (especially Discussion and Confusion).

Computer expert **Johan Mannerskog**, for excellent help with problems in computer programming.

All the staff at the Department of Pathology, Safety assessment, Astra-Zeneca, for giving me help and support through this work. Especially I would like to express my gratitude to **Elisa Basmaci**, for help with staining and sectioning of some of the specimens, **Birgitta Dillner**, for tips and help regarding immunohistochemistry, **Elisabeth Jensen-Lundgren** for sectioning some other specimens, as well as for good work in the image analysis laboratory. **Susanne von Mentzer-Andersson** for help with preparation of biopsies. **Mona Glasare** and **Mait Magnusson** for tips and help regarding histochemical techniques. **Ronny Fransson-Steen**, head of the Department of Pathology, for giving me some time to finish the work, and **Peter Moldéus**, global head of Toxicology, for letting me use the resources at the Safety assessment laboratory.

All my “brothers” at the Sausage Society.

Last, but certainly not least, my family: my parents in law, **Irina** and **Gennadij**, for kindness and comfort during our visits to S:t Petersburg, and for excellent help to retrieve interesting Russian manuscripts. My mother **Barbro** for always believing in me, encouragement and for you always cares. **Elena**, my beloved wife and best companion in life, for endless love, support and encouragement. **Anna**, our lovely daughter, for being the best that happened in my life.

References

- Aherne WA, Dunnill MS. *Morphometry*. 1 ed. London: Edward Arnold, 1982.
- Aguila MB, Pinheiro AR, Parente LB, Mandarim-de-Lacerda CA. Dietary effect of different high-fat diet on rat liver stereology. *Liver International* 2003; 23(5):363-370.
- Albert R, Schindewolf T, Baumann I, Harms H. Three-dimensional image processing for morphometric analysis of epithelium sections. *Cytometry* 1992; 13(7):759-765.
- Albert S, Neill S, Derrick EK, Calonje E. Psoriasis associated with vulval scarring. *Clinical & Experimental Dermatology* 2004; 29(4):354-356.
- Arenson RL, Chakraborty DP, Seshadri SB, Kundel HL. The digital imaging workstation. 1990. *Journal of Digital Imaging* 2003; 16(1):142-162.
- Baak JP. The framework of pathology: good laboratory practice by quantitative and molecular methods. *Journal of Pathology* 2002; 198(3):277-283.
- Baddeley AJ, Gundersen HJ, Cruz-Orive LM. Estimation of surface area from vertical sections. *Journal of Microscopy* 1986; 142(Pt 3):259-276.
- Baddeley AJ. Stereology and survey sampling theory. *Bulletines of the International Statistics Institute, Proceedings 49th session, Florence* 1993; 52:435-449.
- Benedet JL, Wilson PS, Maticic JP. Epidermal thickness measurements in vaginal intraepithelial neoplasia. A basis for optimal CO₂ laser vaporization. *Journal of Reproductive Medicine* 1992; 37(9):809-812.
- Boreham MK, Wai CY, Miller RT, Schaffer JI, Word RA. Morphometric analysis of smooth muscle in the anterior vaginal wall of women with pelvic organ prolapse. *American Journal of Obstetrics & Gynecology* 2002; 187(1):56-63.
- Braendgaard H, Gundersen HJ. The impact of recent stereological advances on quantitative studies of the nervous system. *Journal of Neuroscience Methods* 1986; 18(1-2):39-78.
- Browne J. Georges-Louis Leclerc, Comte de Buffon (1707-88). *Endeavour* 1988; 12(2):86-90.
- Brunetti MM. Critical aspects in the application of the principles of good laboratory practice (GLP). *Annali Dell'Istituto Superiore di Sanita* 2002; 38(1):41-45.
- Bryan RN. The digital rEvolution: the millennial change in medical imaging. *Radiology* 2003; 229(2):299-304.
- Context Vision. *Image Operations Reference Manual*. [No 104708]. 1987. Linköping, Sweden, Context Vision AB.
- Cruz-Orive LM, Weibel ER. Sampling designs for stereology. *Journal of Microscopy* 1981; 122(Pt 3):235-257.
- Danielsson BR, Skold AC, Johansson A, Dillner B, Blomgren B. Teratogenicity by the hERG potassium channel blocking drug almokalant: use of hypoxia marker gives evidence for a hypoxia-related mechanism mediated via embryonic arrhythmia. *Toxicology & Applied Pharmacology* 2003; 193(2): 168-176.

- Delancey JO, Ashton-Miller JA. Pathophysiology of adult urinary incontinence. *Gastroenterology* 2004; 126(1 Suppl 1):S23-S32.
- du Boulay G. Imaging in medicine through the 20th century. *Journal of the Royal College of Physicians of London* 2000; 34(4):357-362.
- Edovitsky E, Elkin M, Zcharia E, Peretz T, Vlodaysky I. Heparanase gene silencing, tumor invasiveness, angiogenesis, and metastasis. *Journal of the National Cancer Institute* 2004; 96(16):1219-1230.
- Eils R, Athale C. Computational imaging in cell biology. *Journal of Cell Biology* 2003; 161(3):477-481.
- Falconer C, Ekman G, Malmstrom A, Ulmsten U. Decreased collagen synthesis in stress-incontinent women. *Obstetrics & Gynecology* 1994; 84(4):583-586.
- Falconer C, Ekman-Ordeberg G, Blomgren B, Johansson O, Ulmsten U, Westergren-Thorsson G et al. Paraurethral connective tissue in stress-incontinent women after menopause. *Acta Obstetrica et Gynecologica Scandinavica* 1998; 77(1):95-100.
- Fu X, Siltberg H, Johnson P, Ulmsten U. Viscoelastic Properties and Muscular Function of the Human Anterior Vaginal Wall. *International Urogynecology Journal* 1995; 6:229-234.
- Gardella D, Hatton WJ, Rind HB, Rosen GD, von Bartheld CS. Differential tissue shrinkage and compression in the z-axis: implications for optical disector counting in vibratome-, plastic- and cryosections. *Journal of Neuroscience Methods* 2003; 124(1):45-59.
- Ghosh D. Francesco Bonaventura Cavalieri (1598-1647). *Indian Journal of Physiology & Pharmacology* 1998; 42(3):319-320.
- Gosline JM, Rosenbloom J. Elastin. In: Piez KA, Reddi AH, editors. *Extracellular Matrix Biochemistry*. New York: Elsevier, 1984: 191-227.
- Gundersen HJ, Bendtsen TF, Korbo L, Marcussen N, Moller A, Nielsen K, Nyengaard JR, Pakkenberg B, Sorensen FB, Vesterby A. Some new, simple and efficient stereological methods and their use in pathological research and diagnosis. *Acta Pathologica et Microbiologica Scandinavica* 1988; 96(5):379-394.
- Gundersen HJG, Boysen M, Reith A. Comparison of semiautomatic digitizer-table and simple point counting performance in morphometry. *Virchows Archiv* 1981; 37:3-45.
- Hameed N. Leiomyoma of the vagina. *Journal of Ayub Medical College, Abbottabad* 2003; 15(2):63-64.
- Haug H, Kuhl S, Mecke E, Sass NL, Wasner K. The significance of morphometric procedures in the investigation of age changes in cytoarchitectonic structures of human brain. *Journal für Hirnforschung* 1984; 25(4):353-374.
- Hedlund M, Granlund GH, Knutsson H. A consistency operation for line and curve enhancement. In: *Proceedings of the IEEE Computer Society Conference on Pattern Recognition and Image Processing*, Las Vegas: 1982.
- Hilliges M, Falconer C, Ekman-Ordeberg G, Johansson O. Innervation of the human vaginal mucosa as revealed by PGP 9.5 immunohistochemistry. *Acta Anatomica* 1995; 153(2):119-126.
- Horobin RW. Biological staining: mechanisms and theory. *Biotechnic & Histochemistry* 2002; 77(1):3-13.
- Howard CV, Reed MG. *Unbiased Stereology; Three-Dimensional Measurement in Microscopy*. 1 ed. New York: Bios publishers, Springer, 1998.
- Hunziker EB, Cruz-Orive LM. Consistent and efficient delineation of reference spaces for light microscopical stereology using a laser microbeam system. *Journal of Microscopy* 1986; 142(Pt 1):95-99.

- James J, Bosch KS, Zuyderhoudt FM, Houtkooper JM, van Gool J. Histophotometric estimation of volume density of collagen as an indication of fibrosis in rat liver. *Histochemistry* 1986; 85(2):129-133.
- James J, Bosch KS, Aronson DC, Houtkooper JM. Sirius red histophotometry and spectrophotometry of sections in the assessment of the collagen content of liver tissue and its application in growing rat liver. *Liver* 1990; 10(1):1-5.
- Jondet M, Dehennin L. Impact of different progestins on endometrial vascularisation of postmenopausal women. A retrospective image analysis-morphometric study. *Maturitas* 2003; 46(3):165-171.
- Kalra MK, Maher MM, Blake MA, Lucey BC, Karau K, Toth TL et al. Detection and characterization of lesions on low-radiation-dose abdominal CT images postprocessed with noise reduction filters. *Radiology* 2004; 232(3):791-797.
- Karlsson LM, Cruz-Orive LM. The new stereological tools in metallography: estimation of pore size in aluminium. *Journal of Microscopy* 1991; 165:391-415.
- Knutsson H. Filtering and reconstruction in image processing. Linköping University, Sweden, 1982.
- Landmann L, Marbet P. Colocalization analysis yields superior results after image restoration. *Microsc Res Tech* 2004; 64(2):103-112.
- Leder O. Sampling techniques in quantitative morphology. *Microscopica Acta - Supplement* 1979;(3):129-138.
- Lopez-De Leon A, Rojkind M. A simple micromethod for collagen and total protein determination in formalin-fixed paraffin-embedded sections. *Journal of Histochemistry & Cytochemistry* 1985; 33(8):737-743.
- Lyon HO, De Leenheer AP, Horobin RW, Lambert WE, Schulte EK, Van Liedekerke B et al. Standardization of reagents and methods used in cytological and histological practice with emphasis on dyes, stains and chromogenic reagents. *Histochemical Journal* 1994; 26(7):533-544.
- Ma T, Cai Z, Wellman SE, Ho IK. A quantitative histochemistry technique for measuring regional distribution of acetylcholinesterase in the brain using digital scanning densitometry. *Analytical Biochemistry* 2001; 296(1):18-28.
- Marotta M, Martino G. Sensitive spectrophotometric method for the quantitative estimation of collagen. *Analytical Biochemistry* 1985; 150(1):86-90.
- Minamitani T, Ikuta T, Saito Y, Takebe G, Sato M, Sawa H et al. Modulation of collagen fibrillogenesis by tenascin-X and type VI collagen. *Experimental Cell Research* 2004; 298(1):305-315.
- Mints M, Blomgren B, Falconer C, Palmblad J. Expression of the vascular endothelial growth factor (VEGF) family in human endometrial blood vessels. *Scandinavian Journal of Clinical & Laboratory Investigation* 2002; 62(3):167-175.
- Mixdorf MA, Goldsworthy RE. A history of computers and computerized imaging. *Radiologic Technology* 1996; 67(4):291-296.
- Møller A, Strange P, Gundersen HJ. Efficient estimation of cell volume and number using the nucleator and the disector. *Journal of Microscopy* 1990; 159(Pt 1):61-71.
- Moore K.L. Clinically oriented anatomy. 3 ed. Baltimore: The Williams & Wilkins company, 1982.
- Moragas A, Castells C, Sans M. Mathematical morphologic analysis of aging-related epidermal changes. *Analytical & Quantitative Cytology & Histology* 1993; 15(2):75-82.
- Morgan DM, Iyengar J, Delancey JO. A technique to evaluate the thickness and density of nonvascular smooth muscle in the suburethral fibromuscular layer. *American Journal of Obstetrics & Gynecology* 2003; 188(5):1183-1185.

- Nichols DH, Randall CL. Vaginal surgery. Baltimore / London: Williams & Wilkins, 1983.
- Nilsson K, Risberg B, Heimer G. The vaginal epithelium in the postmenopause--cytology, histology and pH as methods of assessment. *Maturitas* 1995; 21(1):51-56.
- Olenius M, Forslind B, Johansson O. Morphometric evaluation of collagen fibril dimensions in expanded human breast skin. *International Journal of Biological Macromolecules* 1991; 13(3):162-164.
- Olenius M, Johansson O. Variations in epidermal thickness in expanded human breast skin. *Scandinavian Journal of Plastic & Reconstructive Surgery & Hand Surgery* 1995; 29(1):15-20.
- Pakkenberg B, Gundersen HJ. Total number of neurons and glial cells in human brain nuclei estimated by the disector and the fractionator. *Journal of Microscopy* 1988; 150(Pt 1):1-20.
- Papa Petros PE, Ulmsten U. Role of the pelvic floor in bladder neck opening and closure II: vagina. *International Urogynecology Journal* 1997; 8(2):69-73.
- Peterson DA. Quantitative histology using confocal microscopy: implementation of unbiased stereology procedures. *Methods* 1999; 18(4):493-507.
- Petros PE, Ulmsten UI. An integral theory of female urinary incontinence. Experimental and clinical considerations. *Acta Obstetrica et Gynecologica Scandinavica - Supplement* 1990; 153:7-31.
- Prockop DJ, Kivirikko KI. Collagens: molecular biology, diseases, and potentials for therapy. *Annual Review of Biochemistry* 1995; 64:403-434.
- Purtle HR. History of the microscope. In: Hansen JL, Schrader jr. WA, Cowan WR, editors. *The Billings Microscope Collection*. Washington: Armed Forces Institute of Pathology, 1974: x-xviii.
- Reiffenstahl G, Platzer W, Friedman EA. Atlas of vaginal surgery. Philadelphia / London / Toronto: Saunders, 1975.
- Roberts N, Cruz-Orive LM, Reid NM, Brodie DA, Bourne M, Edwards RH. Unbiased estimation of human body composition by the Cavalieri method using magnetic resonance imaging. *Journal of Microscopy* 1993; 171(Pt 3):239-253.
- Ross MH, Romrell L.J. Histology, a text and atlas. 2 ed. Baltimore: Williams & Wilkins, 1989.
- Roughley PJ. Articular cartilage matrix changes with aging. Buckwater JA, Goldberg VM, Woo SL-Y, editors. *American academy of orthopaedic surgeons symposium*, 1992.
- Royet JP. Stereology: a method for analyzing images. *Progress in Neurobiology* 1991; 37(5):433-474.
- Russ JC. *The Image Processing Handbook*. 2 ed. Boca Raton: CRC press, 1995.
- Saatci E, Tavsanoğlu V. Fingerprint image enhancement using CNN filtering techniques. *International Journal of Neural Systems* 2003; 13(6):453-460.
- Sanders JE, Goldstein BS, Leotta DF, Richards KA. Image processing techniques for quantitative analysis of skin structures. *Computer Methods and Programs in Biomedicine* 1998; 59:167-180.
- Sator PG, Schmidt JB, Sator MO, Huber JC, Honigsmann H. The influence of hormone replacement therapy on skin ageing: a pilot study. *Maturitas* 2001; 39(1):43-55.
- Sterio DC. The unbiased estimation of number and sizes of arbitrary particles using the disector. *Journal of Microscopy* 1984; 134(Pt 2):127-136.
- Sutou D, Akiyama K, Yabe K. A novel technique for quantitative immunohistochemical imaging of various neurochemicals in a multiple-stained brain slice. *Journal of Neuroscience Methods* 2002; 118(1):41-50.

- Techavipoo U, Chen Q, Varghese T, Zagzebski JA, Madsen EL. Noise reduction using spatial-angular compounding for elastography. *IEEE Transactions on Ultrasonics Ferroelectrics & Frequency Control* 2004; 51(5):510-520.
- Ulmsten U. Some reflections and hypotheses on the pathophysiology of female urinary incontinence. *Acta Obstetrica et Gynecologica Scandinavica - Supplement* 1997; 166:3-8.
- Ulmsten U, Falconer C. Connective tissue in female urinary incontinence. *Current Opinion in Obstetrics & Gynecology* 1999; 11(5):509-515.
- van der Rest M, Garrone R. Collagen family of proteins. *FASEB Journal* 1991; 5(13):2814-2823.
- Voipio SK, Komi J, Kangas L, Halonen K, DeGregorio MW, Erkkola RU. Effects of ospemifene (FC-1271a) on uterine endometrium, vaginal maturation index, and hormonal status in healthy postmenopausal women. *Maturitas* 2002; 43(3):207-214.
- Waarsing JH, Day JS, Weinans H. An improved segmentation method for in vivo micro CT imaging. *Journal of Bone and Mineral Research* 2004; 10:1640-1650.
- Wei JT, DeLancey JO. Functional anatomy of the pelvic floor and lower urinary tract. *Clinical Obstetrics and Gynecology* 2004; 47(1):3-17.
- Weibel E.R. *Stereological methods. I. Practical methods for biological morphometry.* London: Academic Press, 1979.
- Weigert C. Über eine methode zur Färbung elastischer Fasern. *Zentralblatt für Allgemeine Pathologie und Pathologische Anatomie* 1898; 9:289.
- Whitmore SE, Levine MA. Risk factors for reduced skin thickness and bone density: possible clues regarding pathophysiology, prevention, and treatment. *Journal of the American Academy of Dermatology* 1998; 38(2 Pt 1):248-255.
- Wicksell SD. The corpuscle problem. A mathematical study of a biometric problem. *Biometrika* 1925; 17:84-99.
- Wilkinson EJ. Normal histology and nomenclature of the vulva, and malignant neoplasms, including VIN. *Dermatologic Clinics* 1992; 10(2):283-296.
- Wulfsohn D, Nyengaard JR, Tang Y. Postnatal growth of cardiomyocytes in the left ventricle of the rat. *Anat Rec* 2004; 277A(1):236-247.
- Zhang DQ, Chen SC. A novel kernelized fuzzy C-means algorithm with application in medical image segmentation. *Artificial Intelligence in Medicine* 2004; 32(1):37-50.

Appendix

Appendix 1 Staining methods

Haematoxylin and Eosin (Harris)

5. Dewax, hydration to dist. water
6. Harris haematoxylin 5-10 min.
7. Rinse in tap water
8. Differentiate in 1% acid alcohol
9. Rinse in tap water
10. Continue until sections 'blue' for 5 min.
11. 1% eosin 5 min.
12. Dehydration in alcohols (70%, 95%, Absolute)
13. Sections to xylene and mount

Weigerts elastin (without Van Gieson counterstain)

1. Dewax, hydration to dist. water
2. Weigerts resorcin-fuchsin 20-45 min.
3. Sections to running tap water 1 min.
4. Weigerts haematoxylin 10 min.
5. Rinse in tap water
6. Differentiate in 1% acid alcohol
7. 70% alcohol
8. 70% alcohol + 3 drops NH_3
9. Rinse in 70% alcohol
10. Rinse in running tap water; examine under microscope
11. Dehydration in 95% alcohol
12. Sections to xylene and mount

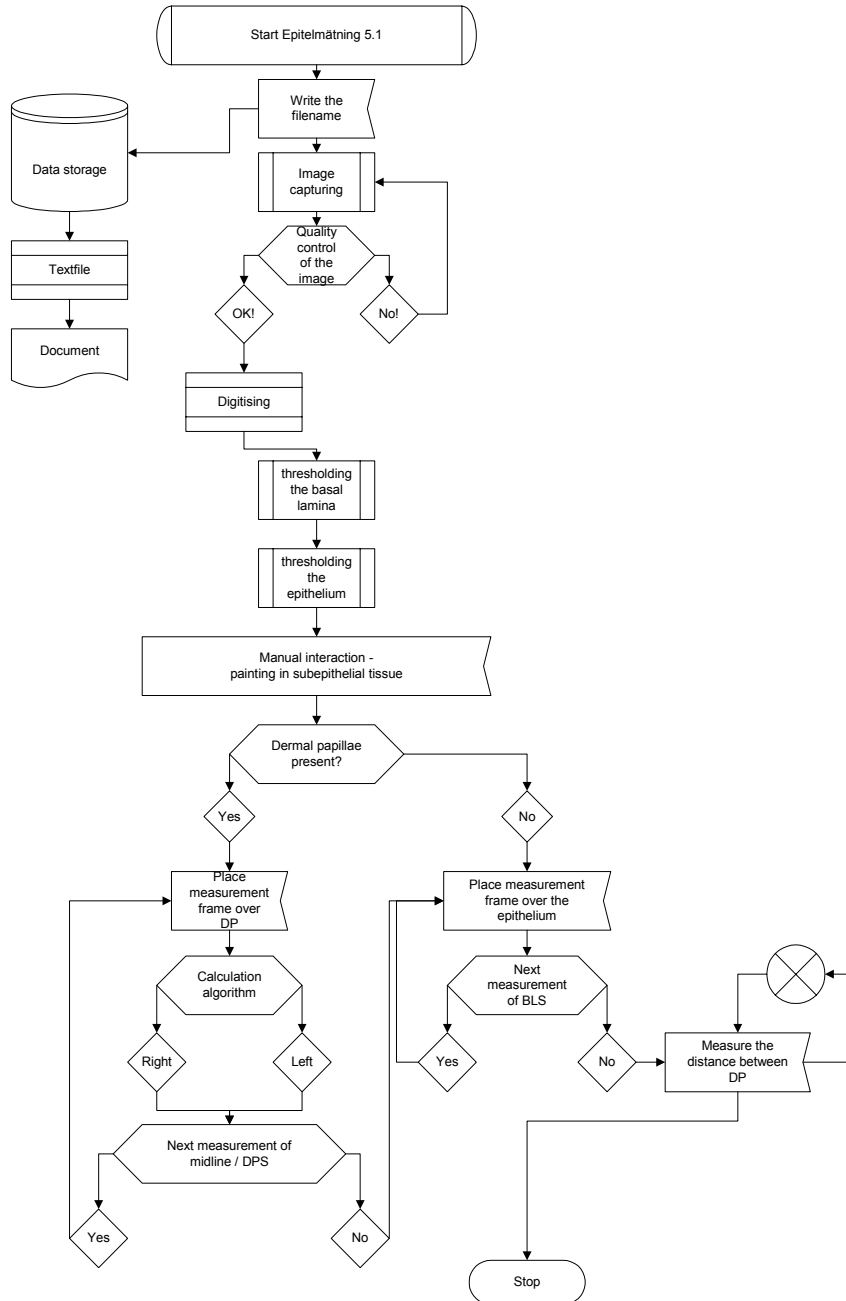
Massons trichrome

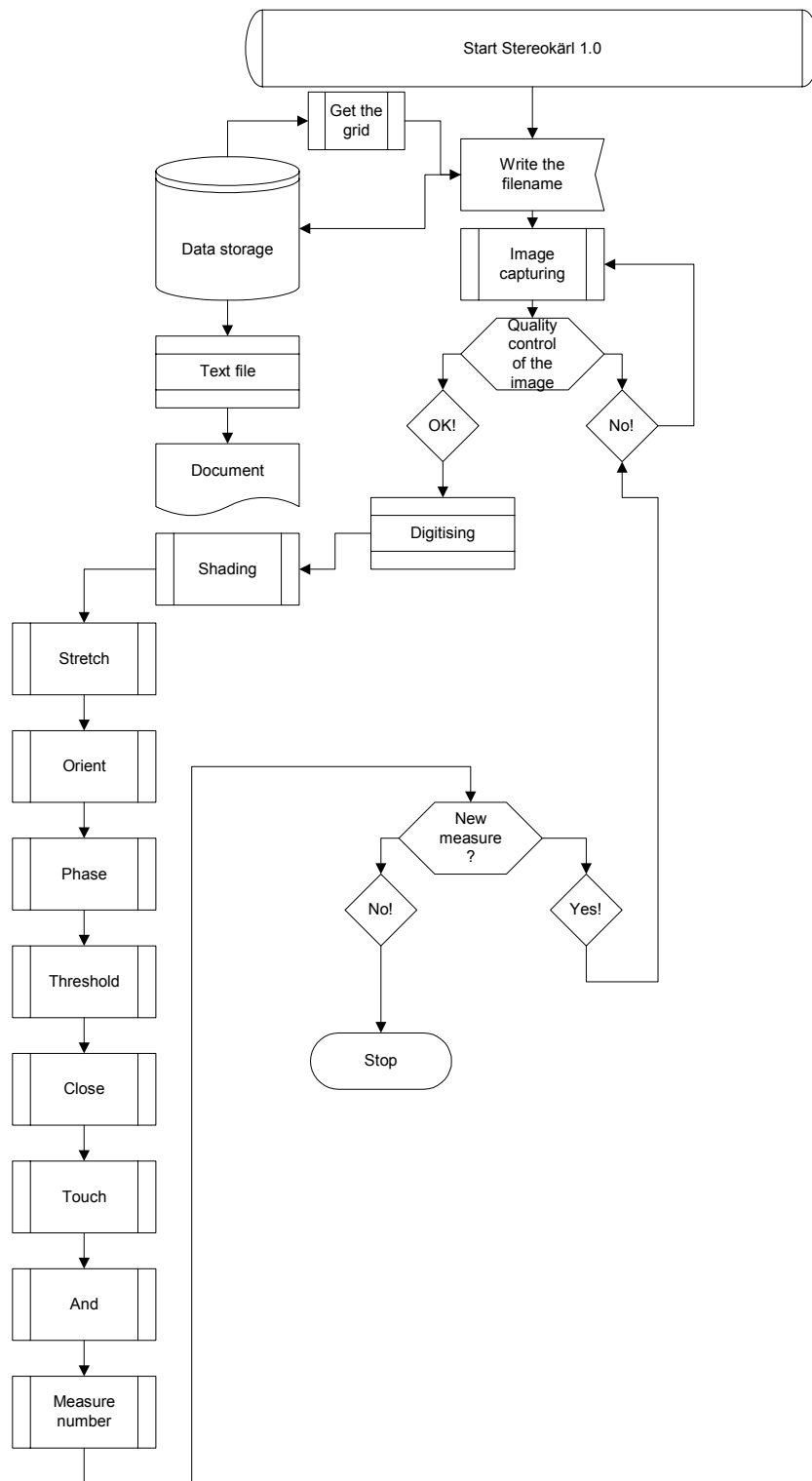
1. Dewax, hydration to dist. water
2. Rinse in distilled water
3. Fixation in Bouins fixative overnight
4. Sections to tap water until the colour has disappeared
5. Rinse in dist. water
6. Weigerts haematoxylin 10 min.
7. Tap water 10 min.
8. Distilled water
9. Biebrich Scarlet-acid-fuchsin solution 15 min.
10. Distilled water
11. Phosphomolybdic-phosphotungstic acid 10-15 min.
12. Methyl blue solution 5-10 min.
13. Distilled water
14. 1% acetic acid 3-5 min.
15. Dehydration in 95% alcohol
16. Sections to xylene and mount

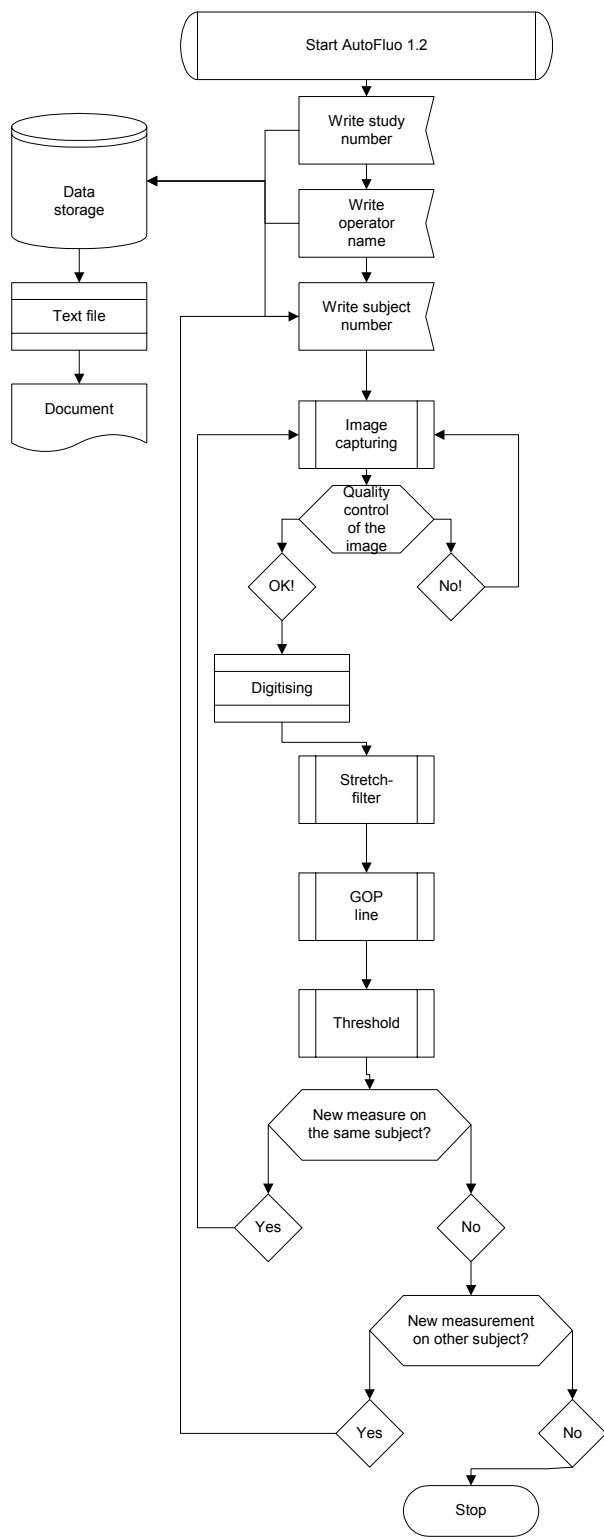
Sirius red

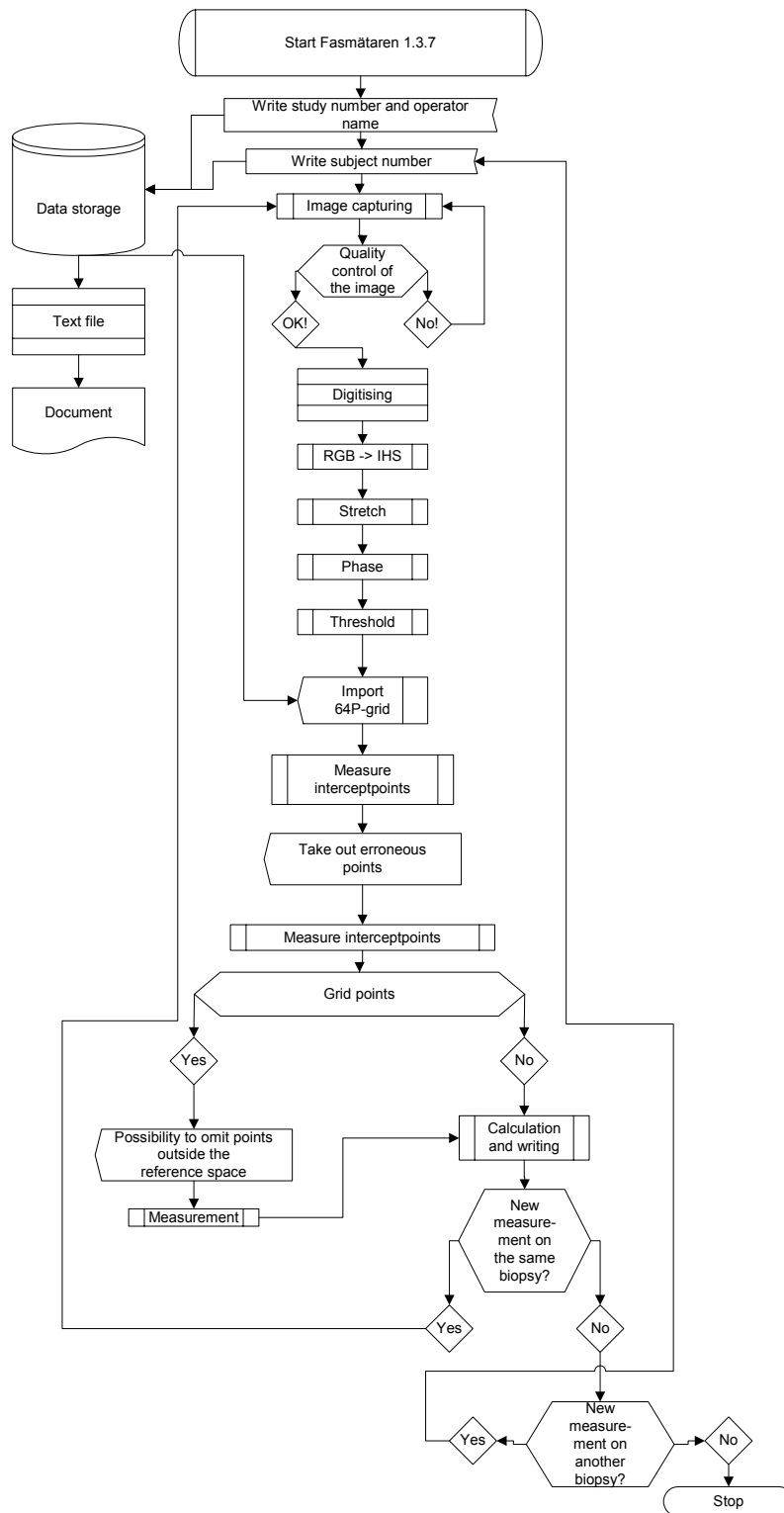
1. Dewax and rehydration
2. Picosirius solution 1 h.
3. Rinse in 0.01 N HCl 2 min.
4. 70% alcohol
5. 95% alcohol
6. Absolute alcohol
7. Sections to xylene and mount

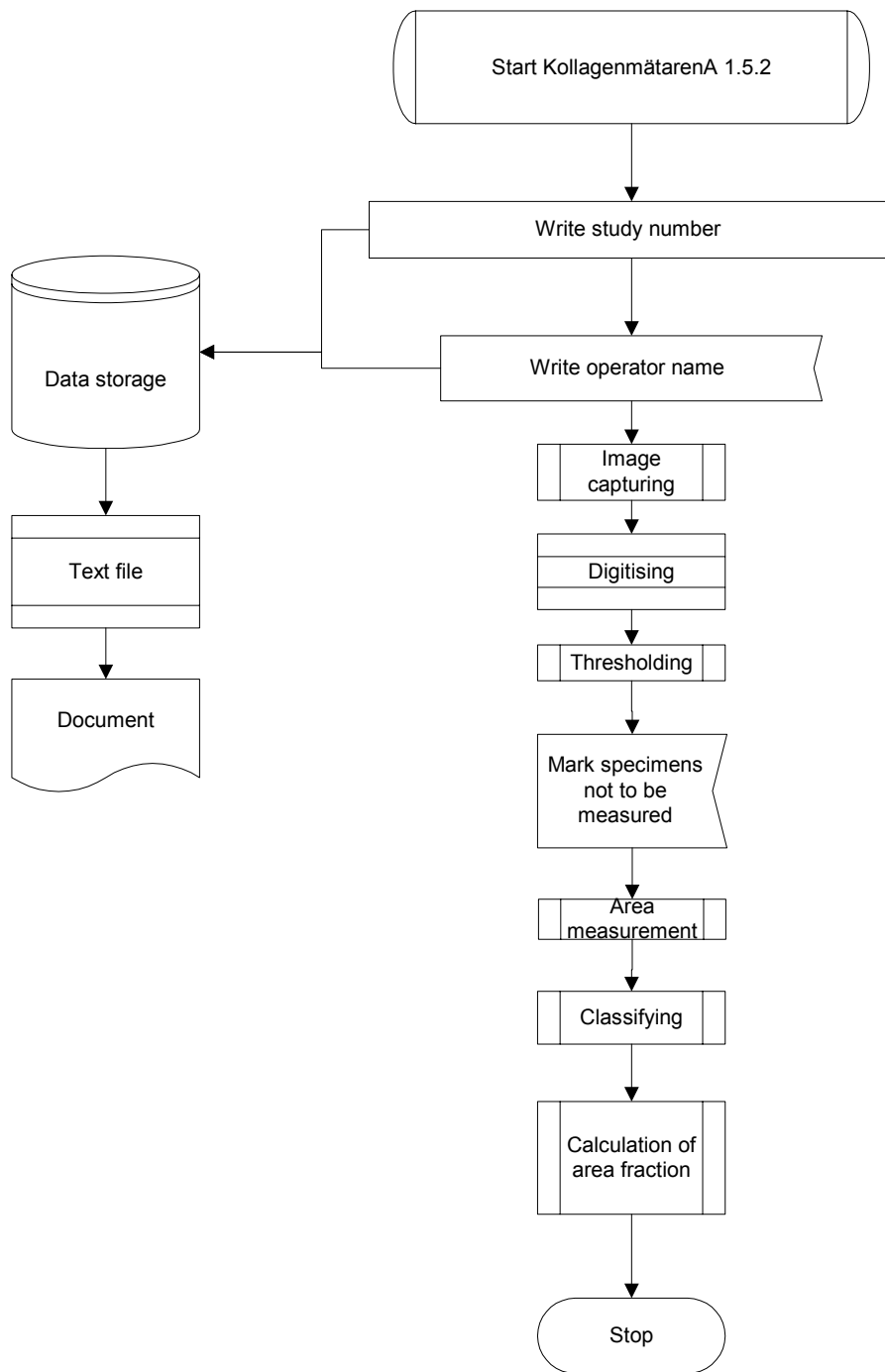
Appendix 2 Computer program flowcharts











Acta Universitatis Upsaliensis

*Comprehensive Summaries of Uppsala Dissertations
from the Faculty of Medicine*

Editor: The Dean of the Faculty of Medicine

A doctoral dissertation from the Faculty of Medicine, Uppsala University, is usually a summary of a number of papers. A few copies of the complete dissertation are kept at major Swedish research libraries, while the summary alone is distributed internationally through the series *Comprehensive Summaries of Uppsala Dissertations from the Faculty of Medicine*. (Prior to October, 1985, the series was published under the title “Abstracts of Uppsala Dissertations from the Faculty of Medicine”.)

Distribution:
Uppsala University Library
Box 510, SE-751 20 Uppsala, Sweden
www.uu.se, acta@ub.uu.se

ISSN 0282-7476
ISBN 91-554-6068-2